AWARD NUMBER: W81XWH-13-1-0200

TITLE: Role of Klotho in Osteoporosis and Renal Osteodystrophy

PRINCIPAL INVESTIGATOR: Beate Lanske

CONTRACTING ORGANIZATION: Harvard University, Boston, MA 02115

REPORT DATE: October 2014

TYPE OF REPORT: Annual

PREPARED FOR: U.S. Army Medical Research and Materiel Command
Fort Detrick, Maryland 21702-5012

REPORT DOCUMENTATION PAGE

Form Approved
OMB No. 0704-0188

1. REPORT DATE	2. REPORT TYPE	3. DATES COVERED
October 2014	Annual	30 Sep 2013 - 29 Sep 2014

4 TITLE AND SUBTITLE
Role of Klotho in Osteoporosis and Renal Osteodystrophy

5a. CONTRACT NUMBER

5b. GRANT NUMBER
W81XWH-13-1-0200

5c. PROGRAM ELEMENT NUMBER

6. AUTHOR(S)
Beate Lanske

E-Mail: beate_lanske@HSDM.Harvard.edu

5d. PROJECT NUMBER

5e. TASK NUMBER

5f. WORK UNIT NUMBER

7. PERFORMING ORGANIZATION NAME(S) AND ADDRESS(ES) AND ADDRESS(ES)
President & Fellows of Harvard College
Sponsored Programs Administration, 25 Shattuck St., Boston Ma 02115
Harvard School of Dental Medicine
188 Longwood Ave
Boston Ma 02115

8. PERFORMING ORGANIZATION REPORT NUMBER

9. SPONSORING / MONITORING AGENCY NAME(S) AND ADDRESS(ES)
U.S. Army Medical Research and Materiel Command
Fort Detrick, Maryland 21702-5012

10. SPONSOR/MONITOR'S ACRONYM(S)

11. SPONSOR/MONITOR'S REPORT NUMBER(S)

12. DISTRIBUTION / AVAILABILITY STATEMENT
Approved for Public Release; Distribution Unlimited **(**

13. SUPPLEMENTARY NOTES

14. ABSTRACT
The most significant findings to date are from mice with Klotho ablated specifically from long bones. First, we found that loss of Klotho in bone disrupts normal bone development. Histological analyses showed that bones of 6-week old *Prx1cre;Klotho*$^{fl/fl}$ mice have normal cortical bone but scarce trabeculae relative to controls. In particular, male *Prx1cre;Klotho*$^{fl/fl}$ mice had reduced bone volume/total volume. The loss was more pronounced at 6 than 24 weeks. This effect was confirmed by *in vitro* analysis with isolated primary osteoblasts treated to delete Klotho that exhibited a defect in bone mineralization. Moreover, male *Prx1cre;Klotho*$^{fl/fl}$ mice have significantly higher expression of all bone formation markers analyzed than controls. Second, we found that bone morphology in mice with induced CKD was more affected in mice without Klotho expression in long bones. The phenotypic changes in the skeleton of CKD mice were consistent with rickets/osteomalacia, but the long bones of *Prx1cre;Klotho*$^{fl/fl}$ mice with CKD were significantly more compromised than those of controls. Also, CKD *Prx1cre;Klotho*$^{fl/fl}$ mice did not exhibit the expected increase in bone formation markers that was observed in CKD control mice. The results provide new insight into the limb specific role of Klotho.

15. SUBJECT TERMS
Klotho, FGF23, PTH, CKD-MBD, Osteoporosis, Mineral Homeostasis, osteopontin, adenine, resorption, FGFR1, ablation, renal failure, parathyroid gland, kidney, bone, phosphate, calcium, uremia.

16. SECURITY CLASSIFICATION OF:			17. LIMITATION OF ABSTRACT	18. NUMBER OF PAGES	19a. NAME OF RESPONSIBLE PERSON
a. REPORT	b. ABSTRACT	c. THIS PAGE			USAMRMC
Unclassified	Unclassified	Unclassified	Unclassified	41	19b. TELEPHONE NUMBER *(include area code)*

Table of Contents

1. Introduction

We are conducting a study regarding the underlying genetic and endocrine mechanisms for Osteoporosis and Related Bone Disease such as skeletal mineralization defects related to chronic kidney failure. Osteoporosis is a significant health problem. It is estimated that 44 million Americans, nearly 70% of which are women, are affected by this disease. It is of particular concern to the Veteran's Administration since women are now the fastest growing segment of veterans. Our work and the work of others have revealed much about the complex physiology of bone development and maintenance including the endocrine regulation of mineral homeostasis that is absolutely necessary for skeletal health. Hormonal factors from bone, kidneys and parathyroid glands form an interactive network to maintain a tight balance of minerals in the body. Our proposal is to develop a better understanding of how one protein in particular, Klotho, specifically contributes to bone mineralization defects. We hypothesize that tissue-specific reduced expression of Klotho is responsible for the bone mineralization defects present in patients with osteoporosis and/or chronic kidney disease. To investigate this hypothesis we have experimentally deleted Klotho expression in parathyroid glands, kidneys, and bone independently to determine 1) how each organ contributes to the disease processes and 2) the relative contribution of each organ to the mineralization defects. We are using our transgenic mouse that utilizes Cre-lox technology to selectively ablate Klotho in each organ and analyze the effects to support our hypothesis.

2. Keywords

Klotho, FGF23, PTH, CKD-MBD, Osteoporosis, Mineral Homeostasis, osteopontin, adenine, resorption, FGFR1, ablation, renal failure, parathyroid gland, kidney, bone, phosphate, calcium, uremia.

3. Accomplishments

Major Goals and Tasks

To test our hypothesis and *attain* our overall aim of delineating the tissue-specific role of Klotho in osteoporosis, CKD-MBD and other bone pathology, we proposed the following specific aims. Each aim is designed to study a specific tissue using floxed Klotho (*Klotho$^{fl/fl}$*) mice crossed with a mouse line carrying the Cre recombinase gene driven by a tissue specific promoter. Mice from these crosses have Klotho ablated from the target tissue by Cre-LoxP recombination.

SA1: Parathyroid gland-specific deletion of Klotho: Klotho has been reported to mediate the suppression of PTH by FGF23. In addition, Klotho has been shown to recruit the Na+,K+-ATPase to the cell surface upon changes in calcium concentrations in the parathyroid gland. It has been suggested that a decrease in Klotho expression in the parathyroid gland is responsible for the induction of secondary hyperparathyroidism due to a resistance to FGF23 suppression of PTH transcription/secretion in CKD-MBD. Specific deletion of *Klotho* from the parathyroid gland is therefore an important prerequisite to obtain novel information about Klotho's organ-specific function in mineral ion homeostasis. *Klotho$^{fl/fl}$* mice will be crossed with *PTHcre* mice to generate mice with Klotho specifically ablated in the parathyroid glands. We will compare *PTHcre;Klotho$^{fl/fl}$* and their control *Klotho$^{fl/fl}$* littermates under normal conditions and then under disease conditions by feeding them an Adenine diet or optionally by 5/6 nephrectomy to induce CKD. The results obtained from this study will provide evidence whether Klotho signaling in the parathyroid glands has a critical role in bone mineral defects.

SA2: Kidney-specific deletion of Klotho: Renal expression of Klotho is important for normal mineral ion homeostasis. To examine the consequence of loss of renal Klotho function from the entire kidney, *Klotho$^{fl/fl}$* mice will be crossed with *Six2cre* transgenic mice; Jax #009606-Six2-EGFP/cre1Amc/J. Six2-expressing cap mesenchyme represents a multipotent nephron progenitor population; therefore deletion of Klotho is anticipated throughout the kidney. Moreover, we plan to refine our data to determine whether Klotho expression in proximal or distal tubules is more critical for CKD-MBD. We have recently demonstrated that Klotho is expressed not only in distal tubules but also in proximal tubules of the kidney. This is an important finding because prior to these data it was unclear how Fgf23 could downregulate the sodium phosphate co-transporters (NaPi2a, NaPi2c) and inhibit expression of the 1α(OH)ase in proximal tubules if Klotho was expressed only in distal tubules. We will investigate the importance of Klotho functions in both tubules by separately ablating Klotho from each cell type. In order to identify Klotho's potential role in proximal tubules to regulate phosphate and vitamin D homeostasis, *Klotho$^{fl/fl}$* mice will be crossed with kidney androgen-regulated protein (*KAP)cre* transgenic mice. To investigate Klotho's function in distal tubules where it has been reported to induce renal calcium re-absorption by its actions on TRPV5 *Klotho$^{fl/fl}$* mice were crossed with mouse cadherin 16 (*Ksp 1.3 kb);cre* mice (article published by JASN; see preliminary data). Induction of CKD in this mouse strain will determine whether renal Klotho is involved in the progression of bone mineralization defects and to what extent this involvement derives from the proximal versus distal tubules. We will compare kidney-specific *cre;Klotho$^{fl/fl}$* and their control *Klotho$^{fl/fl}$* littermates under normal conditions and then under disease conditions by feeding them an Adenine diet or optionally by 5/6 nephrectomy to induce CKD. The results obtained from this study will provide evidence whether Klotho signaling in the kidney has a critical role.

SA3: Bone-specific deletion of Klotho: We and others have recently found that Klotho is expressed at low levels in osteoblasts and that *Klotho$^{-/-}$* mice exhibit a severe mineralization defect *in vivo* and *in vitro*. Most importantly, we have recently discovered that Klotho and PTH function independently of FGF23 to affect bone mineralization. To determine the mechanism that underlies this previously unknown function of Klotho in bone mineralization, we will cross *Klotho$^{fl/fl}$* mice with various cre transgenic mice (*Prx1cre, Col 1(α1)cre, and DMP1cre)* to generate mice with Klotho specifically ablated in the bone. The result obtained from this study will elucidate whether loss of Klotho expression from bone contributes to the mineralization defect observed in osteoporosis, CKD-MBD and other diseases. We will compare bone-specific *cre;Klotho$^{fl/fl}$* and their control *Klotho$^{fl/fl}$* littermates under normal conditions and then under disease conditions by feeding them an Adenine

diet or optionally by 5/6 nephrectomy to induce CKD. The results obtained from this study will provide evidence whether Klotho signaling in the bone has a critical role.

The following set of tasks will be performed for each of the transgenic mouse models listed. Note: the tasks are not completely linear and a subsequent task may begin prior to the end of the previous task.

Task 1: Generate/Maintain Mice (6 months)

- Cross *Klotho*$^{fl/fl}$ with appropriate cre transgenic mice to generate required genotypes.
  Aim 1: **PTHcre;Klotho*$^{fl/fl}$ *and Klotho*$^{fl/fl}$ control littermates
  Aim 2: *Six2cre;Klotho*$^{fl/fl}$ *and Klotho*$^{fl/fl}$ control littermates
  KAPcre;Klotho$^{fl/fl}$ *and Klotho*$^{fl/fl}$ control littermates
  **KSPcre;Klotho*$^{fl/fl}$ *and Klotho*$^{fl/fl}$ control littermates
  Aim 3: *Prx1cre;Klotho*$^{fl/fl}$ *and Klotho*$^{fl/fl}$ control littermates
  Col 1(α1)cre;Klotho$^{fl/fl}$ *and Klotho*$^{fl/fl}$ control littermates
  DMP1cre;Klotho$^{fl/fl}$ *and Klotho*$^{fl/fl}$ control littermates
- Confirm ablation of Klotho using immunohistochemistry and qPCR
- Maintain breeding pairs/Breed experimental mice as needed
  6 mice, both males and females, at birth-P2, 3, 6-9 weeks, and 22 weeks postnatally

  *NOTE: The *PTHcre;Klotho*$^{fl/fl}$ and *KspCre;Klotho*$^{fl/fl}$ mouse lines were generated and characterized prior to the start of the project, but had not been challenged with induction of CKD.

Task 2: Analyze/Compare Mutant Mice to Control Littermates Under Normal Conditions at All Ages (18-21 months)

- *Macroscopic analysis:* morphology, weight, size, survival, health status
- *Biochemical analysis:* serum and urinary parameters
- *Routine Histology:* bone and soft tissues; mineralization (normal and ectopic), proliferation, apoptosis
- *Quantitative analyses:* histomorphometry (bone formation rate/BFR), µCT, or pQCT
- *Gene expression studies:* Nanostring or qRT-PCR in bone, kidney and parathyroid glands
- *Protein expression studies:* Western Blot and Immunohistochemistry in bone, kidney and parathyroids
- *In vitro* analysis: Mineralization using Bone Marrow Stromal Cells and Calvarial Cells, Isolation of Distal Tubular Segments for in vitro analyses
- Statistical Analyses of all Data

Task 3: Challenge Mice with Induction of CKD by either feeding Adenine Diet or 5/6 nephrectomy (7-9 months)

- Produce sufficient litters and genotype all pups
- *Adenine Diet:* Mutant Mice and Klotho$^{fl/fl}$ control mice (see Task 1) will be fed a control diet *(DYETS #I10457 - Modified AIN-76A Purified Rodent Diet with 0.9% Phosphorus and 0.6% Calcium)* with or without addition of adenine for a period of 4 weeks. The mice will start on the diet at weaning (3 weeks old).
- *5/6 nephrectomy:* This procedure will only be performed if the Adenine Diet is not sufficient to induce CKD. We do not expect this since we have already confirmed that the protocol we have established for the Adenine Diet is effective. Nevertheless, as backup plan we would remove 2/3 of the first kidney at between 9-12 weeks of age. The second kidney would be completely removed one week later.
- All Mice will be monitored for adverse side-effects.

Task 4: Analyze Mice Under Disease Conditions (18-21 months)
Subtasks are the same as Task 2 above

Accomplishments

The results of our work for the previous period are summarized here, organized by specific mouse line. Specific target dates were not given in the SOW (see above). We report the percentage of work completed per mouse line based on the task times listed above.

Aim 1 – *PTHCre; Klotho$^{fl/fl}$* Mice

As mentioned in the SOW, much of the work with this mouse line was completed to provide preliminary results for this research proposal. The work was finalized during the first few months of funding and published in December 2013 together with our collaborators (*PLOS Genetics 2013*). *PTHCre;Klotho$^{fl/fl}$* mice have Klotho expression ablated specifically in the parathyroid glands. FGF23, using Klotho as a co-receptor, suppresses PTH production in the parathyroids as part of the regulatory network that controls mineral homeostasis. We found that *PTHCre;Klotho$^{fl/fl}$* mice have normal phenotypes, with normal serum PTH and calcium. Their PTH response to intravenous FGF23 delivery or renal failure did not differ compared to their control littermates despite disrupted FGF23-induced activation of the MAPK/ERK pathway. Further experiments revealed that FGF23 was able to suppress PTH production in the absence of Klotho via an independent, calcineurin-mediated pathway. This is a highly significant, novel finding.

*(Olauson H, Lindberg K, Amin R, Sato T, Jia T, Goetz R, Mohammadi M, Andersson G, **Lanske B**, Larsson TE. Parathyroid-specific deletion of Klotho unravels a novel calcineurin-dependent FGF23 signaling pathway that regulates PTH secretion. PLoS Genet. 2013 Dec;9(12):e1003975).*

Although, this project was considered completed, we were still interested in investigating whether *PTHCre;Klotho$^{fl/fl}$* mice would show an phenotype at an earlier stage in life. Due to the small size of animals at birth (as suggested in the original application, birth – P2) to collect serum and urine, we have chosen to gather the samples at postnatal day 10 (P10). We assumed that at such early stage any potential compensatory mechanisms could be avoided. We could not detect any changes in serum calcium, phosphorous, $1,25(OH)_2D_3$, PTH. Moreover, no changes in urinary calcium or phosphorous could be detected (data not shown). Based on these results, we did not see any reason to continue further investigations and consider this aim as completed.

Aim 2 - *KSPcre;Klotho$^{fl/fl}$* Mice

As noted in the revised SOW, we have dropped this line of mice. This is due to a recent publication on this topic by one of our former collaborators. We believe that it is not necessary to duplicate the study.

(Olauson H, Lindberg K, Amin R, Jia T, Wernerson A, Andersson G, Larsson TE. Targeted deletion of Klotho in kidney distal tubule disrupts mineral metabolism. J Am Soc Nephrol. 2012 Oct;23(10):1641-51).

Aim 2 – *Six2cre;Klotho$^{fl/fl}$* Mice

In collaboration with the Larsson group in Sweden we have generated and characterized *Six2cre;Klotho$^{fl/fl}$* mice. Dr. Olauson has spent some months in my laboratory to work on specific aspects of this project and has finished the analyses back in Sweden at the Karolinska Institute. *Six2cre;Klotho$^{fl/fl}$* mice exhibit a similar phenotype as the global *Klotho* knockout mice. Due to their severe phenotype induction of renal failure was impossible and was therefore not performed. This project is now considered complete and was published in *JASN*.

*(Lindberg K, Amin R, Moe OW, Hu MC, Erben RG, Ostman Wernerson A, **Lanske B**, Olauson H, Larsson TE. The Kidney Is the Principal Organ Mediating Klotho Effects. J Am Soc Nephrol. 2014 Oct;25(10):2169-75).*

Aim 2 - *KAPcre;Klotho$^{fl/fl}$* Mice

While Klotho is expressed mainly in the renal distal tubules, it also expressed at low levels in renal proximal tubules. The function of Klotho in the proximal tubules is to act as a co-receptor for FGF23, which downregulates the sodium phosphate co-transporters (NaPi2a, Napi2c) and inhibits expression of 1α(OH)ase. We are interested in determining if there are any systemic effects on mineral homeostasis specifically due to loss of Klotho in the proximal tubules. In order to explore this, we generated a mouse model in which Klotho is specifically ablated in the proximal tubules. We selected a Cre mouse that uses the Kidney Androgen-regulated Protein (KAP), which is expressed in proximal tubules, to drive the cre recombinase to cross with our floxed Klotho mouse. In order to analyze the recombination specificity and efficiency of the gene ablation, we also

crossed in a mouse with a tdTomato reporter. Male mice were used in preliminary studies but natural levels of testosterone were not sufficient to drive Cre expression to the level needed. We decided to use female mice with artificially increased testosterone levels. Females were subcutaneously implanted with a continuous release testosterone pellet (5mg) at 6 weeks of age. The androgen was released over a 21 day period until the mice were 9 weeks of age. However, we noted that the increase in testosterone levels has an effect on the serum and urine levels of some of the parameters we are studying (such as $1,25(OH)_2D_3$), thus masking the actual effects of Klotho ablation. In order to avoid this problem, mice were maintained without testosterone for an additional five weeks to wash out these effects and mice were sacrificed for analysis at 14 weeks of age.

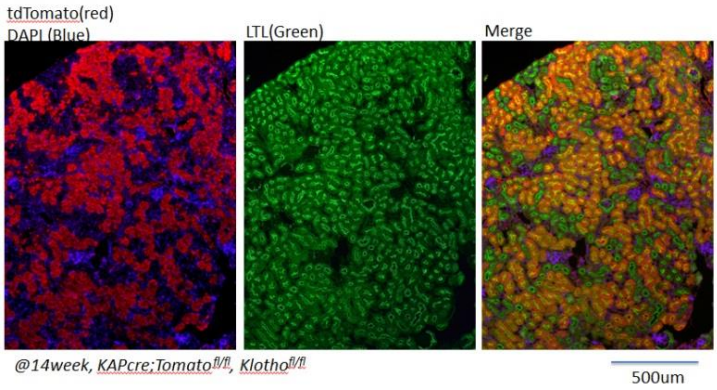

First, we identified the cells that express the Cre recombinase in sections of kidney that were double-stained with *Lotus tetragonolobus* lectin (LTL) that specifically labels differentiated proximal tubule and an anti-Red Fluorescent Protein (RFP) antibody to detect tdTomato protein. The recombination efficiency, as determined by this immunofluorescent analysis of the tdTomato/LTL ratio, was found to be 66% in *KAPcre;Tomato* $^{fl/fl}$*;Klotho* $^{fl/fl}$ mice at 14 weeks of age (Figure 1).

Figure 1: Immunofluorescence: Specific expression of Kapcre (red) in proximal tubules (green) and overlap (yellow).

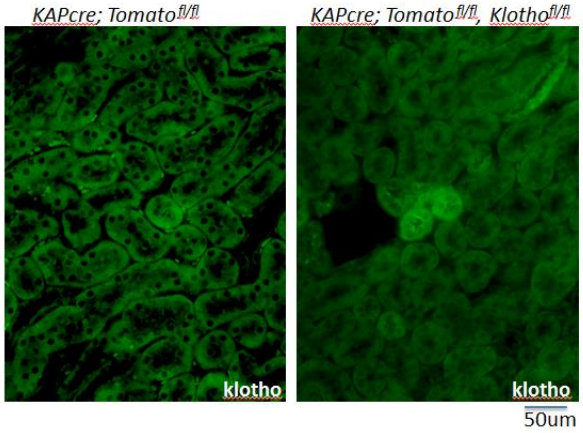

Deletion of Klotho was confirmed using an immunofluorescent approach which showed that Klotho expression was decreased in *KAPcre;Tomato* $^{fl/fl}$*;Klotho* $^{fl/fl}$ mice compared with *KAPcre;Tomato* $^{fl/fl}$ mice (Figure 2).

Figure 2: Efficient deletion of Klotho in *KAPcre; Tomato* $^{fl/fl}$*;Klotho* $^{fl/fl}$ mice is shown by decreased green fluorescence.

Next, we performed an initial mineral metabolism analysis which was expected to show alterations in response to proximal tubules specific Klotho deletion. However, in *KAPcre;Tomato* $^{fl/fl}$*; Klotho* $^{fl/fl}$ mice, there were no significant changes in urine or serum levels of calcium and phosphate (Figure 3).

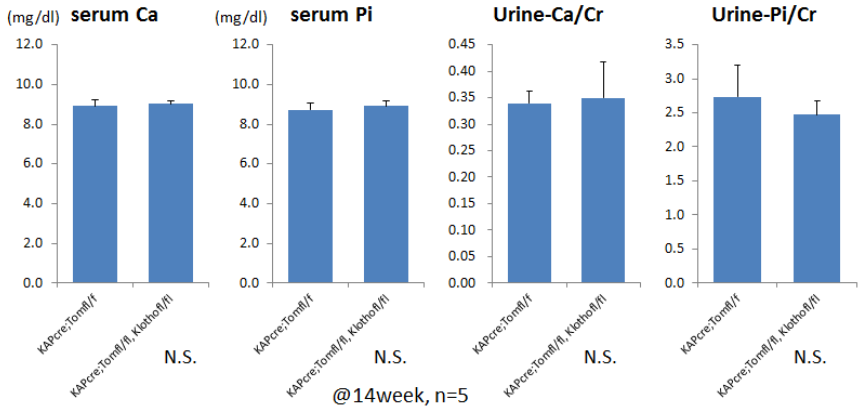

Figure 3: Serum and urine biochemistry of *KAPcre;Tomato* $^{fl/fl}$ *and KAPcre;Tomato* $^{fl/fl}$*; Klotho* $^{fl/fl}$ mice at 14 weeks of age (n=5, N.S. = not significant).

Moreover, the regulatory factors that affect serum calcium and phosphate level were also unchanged with the exception of serum PTH. PTH concentration significantly increases in *KAPcre;Tomato* $^{fl/fl}$*,Klotho* $^{fl/fl}$ mice. However, serum FGF23 and $1,25(OH)_2D_3$ levels did not significantly change, as would have be expected with the observed increase in PTH (Figure 4).

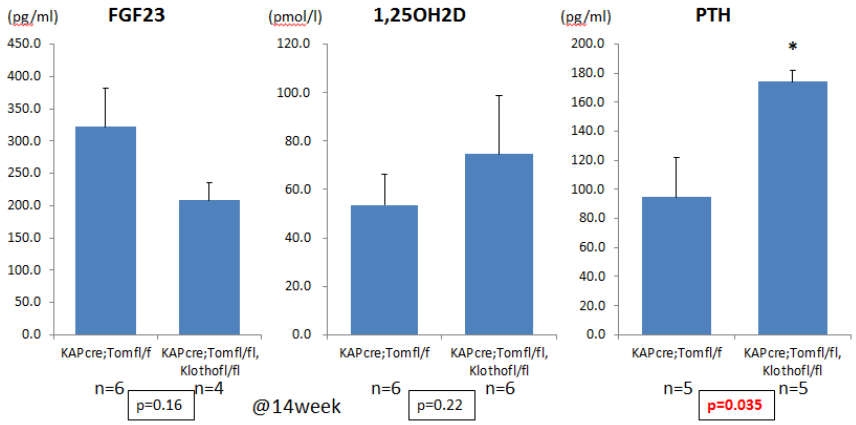

Figure 4: Serum measurements of iFGF23, $1,25(OH)_2D_3$ and PTH. (n=4-6, $p<0.05$).

FGF23/FGFR1/Klotho signaling in the proximal tubule is an inhibitory regulator of NaPi2a/NaPi2c proteins and 1alpha-hydroxylase mRNA. As a consequence, NaPi2 protein and function are expected to increase with the loss of Klotho, causing increased Pi uptake and decreased Pi urinary excretion. Also, 1α-hydroxylase mRNA and function should increase, leading to increased $1,25(OH)_2D_3$ production. Surprisingly, these effects were not observed in our *KAPcre;Tomato* $^{fl/fl}$*;Klotho*$^{fl/fl}$ mice. Moreover, serum PTH was significantly increased in the mutant mice, which should have also stimulated 1a-hydroxylase mRNA expression.

The observation regarding PTH levels is of great interest but the lack of change in other parameters like $1,25(OH)_2D_3$ is problematic. The levels of testosterone drop after the washout period but still remain significantly higher than before treatment. This residual effect may be disrupting our measurements. Further, we believe that there is also a compensatory effect that is affecting the results. KAP expression is restricted to only a portion of the proximal tubule and the remaining, unaffected section may be compensating for the loss of Klotho.

To address these potential problems, we have decided to take advantage of a new Cre mouse, *SLC34a1-GFPCreER (*also *SLC34a1*^{GCE}*)*, in which Cre will be expressed in the entire proximal tubule, thus ablating Klotho more efficiently *(Kusaba T, Lalli M, Kramann R, Kobayashi A, Humphreys BD. Differentiated kidney epithelial cells repair injured proximal tubule. Proc Natl Acad Sci U S A. 2014 Jan 28;111(4):1527-32).* The new experimental mouse, *SLC34a1*^{GCE}*;Tomato* $^{fl/fl}$*;Klotho*$^{fl/fl}$, will also have the advantages of being Tamoxifen inducible, equally effective in male and female mice and not require the washout period needed after testosterone treatment.

Aim 3 – *Prx1cre;Klotho*$^{fl/fl}$ Mice

This aim is to investigate how bone-specific changes in Klotho expression affect mineral ion homeostasis and the progression of bone mineralization defects in chronic kidney disease. For this purpose, floxed Klotho mice were crossed with mice expressing Cre recombinase under the control of the Prx1 promoter to create a mouse in which *Klotho* is deleted in early limb mesenchyme.

Validation of membrane-KL inactivation in conditional knockout mice

The genotype of transgenic mice was determined by PCR analysis of genomic DNA isolated from tail biopsies. PCR for the Cre transgene was performed using 5'primer275 (CGC GGT CTG GCA GTA AAA ACT) and 3'primer603 (CCC ACC GTC AGT ACG TGA GAT ATC). PCR for loxP used KL-LoxP forward (TTGTCAATATGTAAATAATTTGAGCAGTAGGG) and KL-LoxP reverse (GTTGTTGAAAGAGGGAGC TAGTGGTAGTTA) primers which produce bands of two sizes. A larger band represents the wild-type allele and the smaller band represents the LoxP allele.

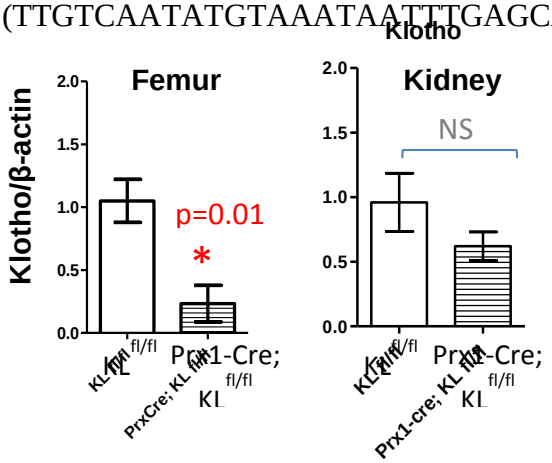

Specific and efficient ablation of Klotho mRNA from long bones of *Prx1cre;Klotho*$^{fl/fl}$ mice was confirmed by qRT-PCR using mRNA extracted from femurs. *Prx1cre;Klotho*$^{fl/fl}$ mice had a 60-70% reduction of Klotho mRNA expression in the cortical shaft of femurs when compared to the Klotho mRNA expression of control littermates (Figure 5). No change in kidney was found.

Figure 5: Deletion of Klotho from long bones but not kidney.

The lack of Klotho protein was confirmed by immunohistochemistry performed on tibias using an anti-Klotho polyclonal antibody (Figure 6). To show Cre specificity, Klotho mRNA expression was measured in the kidney and, as expected, no differences were observed between *Prx1cre;Klotho*$^{fl/fl}$ and *Klotho*$^{fl/fl}$ mice at 6, 16 or 24 weeks of age.

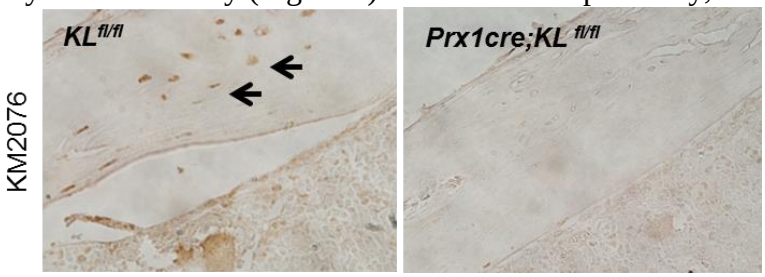

Figure 6: Immunohistochemistry using KM2076 Klotho antibody. Deletion of Klotho from long bones in *Prx1cre;Klotho*$^{fl/fl}$ could be confirmed.

Limb-specific inactivation of membrane Klotho (mb-Klotho) does not alter body size or endocrine regulation

- Macroscopic analyses showed that there were no differences in body weight, body size, or survival rate between *Prx1cre;Klotho*$^{fl/fl}$ and *Klotho*$^{fl/fl}$ mice at P1, 6, 16 or 24 weeks of age (data not shown).
- Biochemical analyses revealed that there were no significant differences in urinary phosphate and/or calcium excretion between *Prx1cre;Klotho*$^{fl/fl}$ and *Klotho*$^{fl/fl}$ mice at 6, 16 or 24 weeks of age. Likewise, there were no differences in serum phosphate, FGF23, parathyroid hormone (PTH) or calcitriol ($1.25(OH)_2D_3$) between genotypes at 6, 16 or 24 weeks of age. Serum calcium was significantly elevated in male and female *Prx1cre;Klotho*$^{fl/fl}$ mice at 6 weeks of age compared to control littermates but no significant changes were observed at 16 or 24 weeks of age suggesting that this may be a transient effect. The absence of endocrine changes in *Prx1cre;Klotho*$^{fl/fl}$ mice (data not shown) is contrary to the endocrine profile of *Klotho* knockout mice, which present with hypercalcemia, hyperphosphatemia, hypoparathyroidism as well as high levels of serum calcitriol and serum iFGF23. Thus, *Prx1cre;Klotho*$^{fl/fl}$ mice provide a good model to investigate the paracrine role of membrane Klotho on development and regulation of bone and mineral metabolism.

Limb-specific inactivation of mb-Klotho disrupts bone development in healthy mice

- X-ray examination along with Alizarin Red/Alcian Blue staining of the skeleton did not reveal obvious skeletal abnormalities in *Prx1cre;Klotho*$^{fl/fl}$ mice at P1 or 6 weeks of age.
- Histological analyses with H&E staining showed that long bones of 6-week old *Prx1cre;Klotho*$^{fl/fl}$ mice have normal cortical bone but scarce trabeculae relative to WT littermates.
- In line with these observations µCT analyses confirmed that there are no changes in cortical bone volume and/or thickness between *Prx1cre;Klotho*$^{fl/fl}$ and *Klotho*$^{fl/fl}$ mice at 6 or 24 weeks of age. Moreover, female *Prx1cre;Klotho*$^{fl/fl}$ mice showed no changed in trabecular bone parameters at 6 or 24 weeks of age. However, as early as 6 weeks of age, male *Prx1cre;Klotho*$^{fl/fl}$ mice had reduced bone volume/total volume (BV/TV). The loss of bone volume was more pronounced at 6 than 24 weeks. Quantitative analyses of µCT reconstructions revealed that the reduced trabecular bone volume is due to reduced bone connectivity (↓Tb. N and ↑Tb.Sp) (Figure 7).

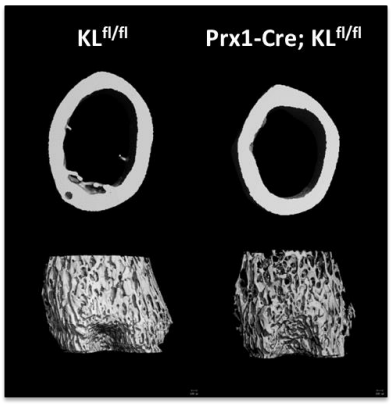

Figure 7: µCT analysis of cortical and trabecular bone (femur) at 6 wks of age. *Prx1cre;Klotho*$^{fl/fl}$ show reduced trabecular BMD with no change in cortical bone.

- To investigate the role of Klotho on bone mineralization we isolated primary osteoblasts from *Klotho*$^{fl/fl}$ mice and treated cells with Adeno-Cre. Deletion of Klotho resulted in a defect in bone mineralization (Figure 8).

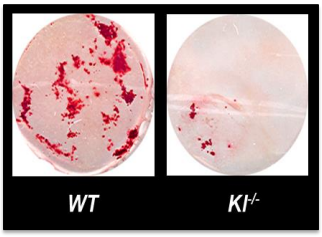

Figure 8: In vitro culture of calvarial osteoblasts under mineralizing conditions.

- Bone mineralization is locally controlled by phosphate regulating molecules including FGF23. Given that Klotho forms a heteromeric complex with FGF23 and FGFR1, it was of interest to investigate whether limb-specific deletion of Klotho affects FGF23 and/or FGFR1 expression. RT-PCR analyses of femur mRNA revealed that the transcript level of FGF23 and FGFR1 in *Prx1cre;Klotho*$^{fl/fl}$ mice was not significantly different from that of control littermates. Moreover, immunohistochemistry and ELISA analyses specific for FGF23 confirmed that the level of intact FGF23 protein in tibia and circulation does not differ between *Prx1cre;Klotho*$^{fl/fl}$ and *Klotho*$^{fl/fl}$ mice at 6 or 24 weeks of age (data not shown).
- The structure of bone depends on an interaction of bone formation and resorption, which are modulated by osteoblasts and osteoclasts, respectively. To better understand how loss of Klotho from mesenchymal stem cells modulates bone, we examined the mRNA expression of genes expressed throughout the evolution of bone cells. RT-PCR analyses of mRNA extracted from the femurs of 6 week old mice revealed that male *Prx1cre;Klotho*$^{fl/fl}$ mice have significantly higher expression of all bone formation markers analyzed (BMP2, Runx2, PTHR1, Osx, Col1a1, ALP, OC, FAM20C, SOST, OPG) than control littermates, with the exception of FGF23 (data not shown).

We then challenged *Prx1cre;Klotho*$^{fl/fl}$ mice with CKD induced by an adenine diet in order to study the effect of ablated Klotho expression in bone under disease conditions.

<u>Implementation and Validation of CKD Model</u>

- We induced renal failure in mice using an adenine diet following a previously published protocol (*Jia T, Olauson H, Lindberg K, Amin R, Edvardsson K, Lindholm B, Andersson G, Wernerson A, Sabbagh Y, Schiavi S, Larsson TE. A novel model of adenine-induced tubulointerstitial nephropathy in mice. BMC Nephrol. 2013 May 30;14:116*). The study was preceded by a 7-day adaptation phase to the casein diet without addition of adenine. Then 8-week old *Prx1cre;Klotho*$^{fl/fl}$ and *Klotho*$^{fl/fl}$ mice were randomized to either a control or adenine enriched diet. Control mice received the casein-based diet without adenine, while experimental mice were exposed to an 8-week protocol to induce renal failure in a mouse model. Briefly, the 8-week protocol included a 10-day induction phase where mice were exposed to 0.3% adenine, and a 7-week maintenance phase with 0.15-0.2% adenine.

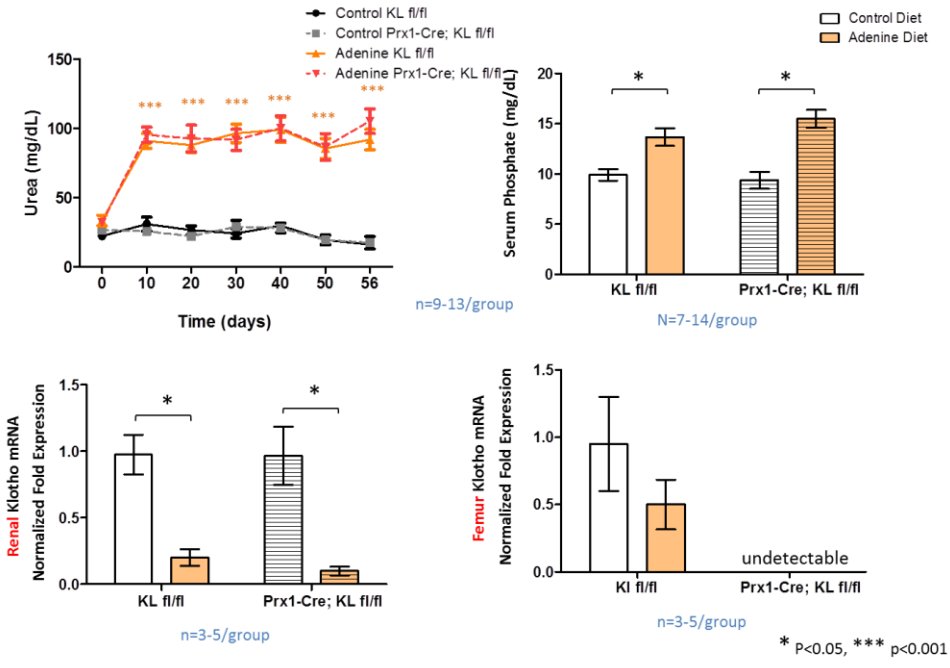

- Similar to CKD patients, *Prx1cre;Klotho*$^{fl/fl}$ and *Klotho*$^{fl/fl}$ mice exposed to adenine-enriched diet had severally damaged kidneys, serum urea levels ranging from 80-100 mg/dL, hyperphosphatemia and secondary hyperparathyroidism. In contrast, control mice exposed to casein-diet without adenine did not exhibit changes in renal histology, serum urea or phosphate levels compared to mice on a regular diet (Figure 9).

<u>Figure 9</u>: Serum Urea, serum phosphate, renal Klotho expression and Klotho expression in femur of *Prx1cre;Klotho*$^{fl/fl}$ and *Klotho*$^{fl/fl}$ mice.

Due to renal damage, both *Prx1cre;Klotho*$^{fl/fl}$ and *Klotho*$^{fl/fl}$ mice had a 70-80% reduction of renal Klotho, PTHR1, NaPi2a and NaPi2c mRNA expression when normalized to the mRNA expression of WT littermates (data not shown). The induction of renal failure significantly reduced the renal Klotho expression in both *Prx1cre; Klotho*$^{fl/fl}$ and *Klotho*$^{fl/fl}$ mice. As expected *Prx1cre;Klotho*$^{fl/fl}$ mice on both control and adenine diet had undetectable levels of Klotho RNA expression in long bones (i.e. femur) while *Klotho*$^{fl/fl}$ mice showed normal expression. (Figure 9).

- There were no significant changes in Klotho mRNA expression at the spine between groups which confirms Cre specificity (data not shown).

Limb-specific Inactivation of Klotho Does Not Alter Body Size in the CKD Mouse Model

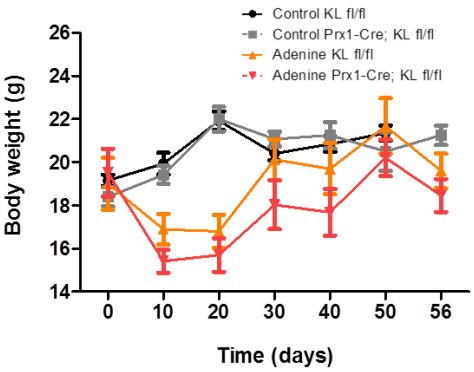

- All adenine fed mice had a significant decline in body weight during the induction phase that stabilized and was essentially unaltered during the maintenance phase. There were no differences in body weight or survival rate between *Prx1cre;Klotho*$^{fl/fl}$ and *Klotho*$^{fl/fl}$ mice on casein diet with or without adenine (Figure 10).

Figure 10: Body weight of 4 groups of mice. Grey lines are mice on control diet, red/orange are mice on adenine diet.

Limb-specific Inactivation of Klotho Disrupts Bone Morphology in the CKD Mouse Model

- Histological analyses with H&E staining showed that tibias and femurs of adenine fed mice have significantly thinner cortical bone with disrupted mineralization and have a pronounced periosteum layer that was filled with densely packed cells. These effects were not seen in control fed mice. The phenotypic changes in the skeleton of the adenine fed mice were consistent with a diagnosis of rickets/osteomalacia. Among the adenine fed mice, long bones of *Prx1cre;Klotho*$^{fl/fl}$ mice were significantly more compromised than those of *Klotho*$^{fl/fl}$ mice, which suggests that Klotho may have a protective role on bone in CKD (Figure 11).

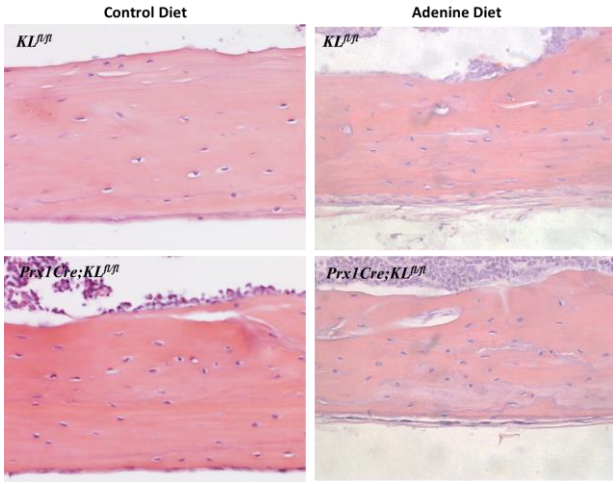

Figure 11: H&E staining of cortical bone of *Klotho*$^{fl/fl}$ and *Prx1cre;Klotho*$^{fl/fl}$ mice on control diet (left) and Adenine diet (right).

- Serum CTX analyses revealed increased bone resorption following adenine exposure with no significant differences between adenine fed *Prx1cre;Klotho*$^{fl/fl}$ and *Klotho*$^{fl/fl}$ mice (data not shown).
- The ratio of RANKL/OPG at the femur (analyzed via RT-PCR) was significantly higher among adenine fed mice than control mice with no significant differences between different genotypes. This confirms that CKD rather than loss of Klotho is responsible for increased bone resorption (data not shown).
- mRNA expression measured using RT-PCR showed that adenine fed *Klotho*$^{fl/fl}$ mice have increased bone formation markers (i.e. Runx2, Osx, Col1a, Osteopontin) in the femur compared to control *Klotho*$^{fl/fl}$ mice. This is expected since increased bone resorption is usually accompanied by increased bone formation. However, adenine fed *Prx1cre;Klotho*$^{fl/fl}$ mice showed no significant increase in these bone formation markers compared to control fed *Prx1cre;Klotho*$^{fl/fl}$*l* mice (data not shown).

- Whole body X-ray imaging revealed that *Prx1cre;Klotho*$^{fl/fl}$ mice exposed to adenine-enriched diet, and not *Klotho*$^{fl/fl}$, have minor scoliosis and severe kyphosis with more pronounced effects in female than male mice (Figure 12).

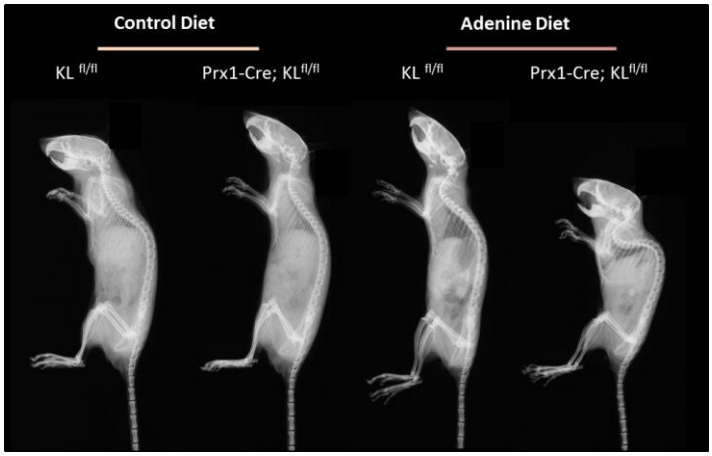

Figure 12: Severe kyphosis of *Prx1cre;Klotho*$^{fl/fl}$ mice after induction of renal failure by adenine diet (mouse to the right).

These phenotypic changes resemble those of *Klotho*$^{-/-}$, *FGF23*$^{-/-}$, *1αOHase*$^{-/-}$, *VDR*$^{-/-}$ *and FAM20c* $^{-/-}$ mice. Since membrane Klotho was only deleted from long bones, the observed changes in spine curvature are believed to be due to secondary effect due to deletion of *Klotho* from long bones indicating some endocrine changes.

- Histomorphometric analyses are currently being processed and analyzed to better understand the overall bone phenotype of *Prx1cre;Klotho*$^{fl/fl}$ mice.

We will continue to analyze these mice and will hopefully summarize all data for a new publication in the near future.

Aim 3 – *DMP1cre;Klotho*$^{fl/fl}$ Mice

Recent experimental data have shown that Klotho is expressed at low levels in osteocytes, but the specific role of Klotho in osteocytes remains unknown. Klotho that is expressed in osteocytes may affect skeletal mineralization and systemic mineral homeostasis. We generated mice with Klotho specifically ablated in osteocytes by crossing *Klotho*$^{fl/fl}$ mice with *DMP1cre* mice to study this possibility. Moreover, emerging data suggest that expressions of Klotho in the kidney and the parathyroid gland are decreased in renal failure and this down-regulation plays an important role in the pathogenesis of CKD-MBD. Thus, we are challenging these mutant mice by performing 5/6 nephrectomy in order to determine the potential role of osteocyte expressed Klotho in disease progression.

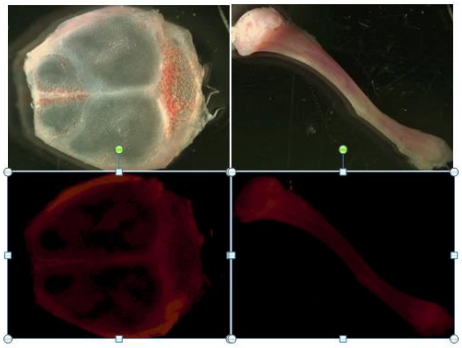

First, we confirmed Dmp1-Cre expression in bone by crossing *DMP1cre* mice with *tdTomato*$^{fl/fl}$ reporter mice. We found that Dmp1-Cre-mediated expression of tdTomato occured in calvaria and long bones (Figure 13).

Figure 13: left: Calvarium of *Dmp1-cre;tdTomato*$^{fl/+}$ mice (top, bright field; bottom, fluorescence); right: Femur of *Dmp1-cre;tdTomato*$^{fl/+}$ mice (top, bright field; bottom, fluorescence).

We found no evidence for the expression of tdTomato in other Klotho-expressing tissues, including the kidney and parathyroid gland. Consistent with these observations, there were marked reductions (~80-90%) in Klotho transcripts in osteocytes but no changes in expression in the kidney or parathyroid glands.

DMP1cre;*Klotho*$^{fl/fl}$ mice were indistinguishable from *Klotho*$^{fl/fl}$ littermates and wild-type mice. In our preliminary analysis, there was no significant difference in serum levels of calcium and phosphorus. We therefore will challenge the mice by inducing renal failure by 5/6 nephrectomy. We have begun this process by testing the technique and verifying renal failure. The procedure is performed in 5 or 6 week-old mice following a two-step surgical procedure. Briefly, the right kidney is exposed, decapsulated, and two-thirds of the kidney is resected. After a 1-week recovery period, a left total nephrectomy is performed. There is an 80% survival rate for nephrectomized mice. After two weeks, BUN is tripled and serum creatinine is doubled in nephrectomized mice (Figure 14), confirming renal failure. The surgery procedure extends the experimental period and the 20%

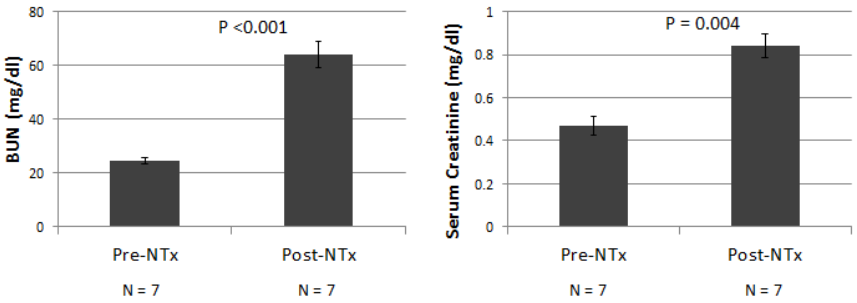

lethality requires extra mice order to have a statistically valid sample for experiments. This has a minor impact on schedules.

Figure 14: serum BUN and creatinine before and 2 weeks after 5/6 NTX.

We have also established a method to specifically isolate osteocytes from mature long bones (Figure 15). This technique will enable us to investigate the function of osteocytes derived from these mutant mice, with or without renal failure, using *in vitro* analysis.

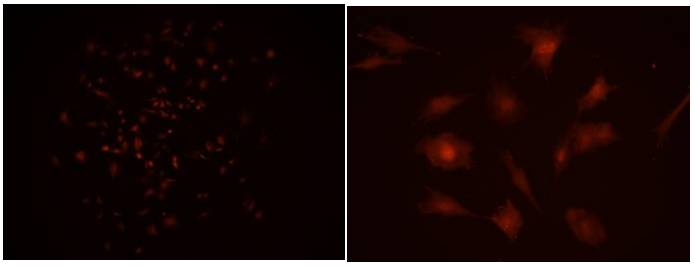

Figure 15: Osteocytes (red) isolated from long bones of *Dmp1-cre;tdTomato*$^{fl/+}$ mice (left, low magnification; right, high magnification).

Aim 3 – *Col 1(α1)cre;Klotho*$^{fl/fl}$ Mice

We are in the process of validating and importing a *Col1(α1)cre* transgenic mouse line (*Liu F, Woitge HW, Braut A, Kronenberg MS, Lichtler AC, Mina M, Kream BE. Expression and activity of osteoblast-targeted Cre recombinase transgenes in murine skeletal tissues. Int J Dev Biol. 2004 Sep;48(7):645-53)* for this portion of the project. We have not begun to cross mice with the floxed Klotho line. We are also considering the use of a *Runx2cre* transgenic mouse *(Rauch A, Seitz S, Baschant U, Schilling AF, Illing A, Stride B, Kirilov M, Mandic V, Takacz A, Schmidt-Ullrich R, Ostermay S, Schinke T, Spanbroek R, Zaiss MM, Angel PE, Lerner UH, David JP, Reichardt HM, Amling M, Schütz G, Tuckermann JP. Glucocorticoids suppress bone formation by attenuating osteoblast differentiation via the monomeric glucocorticoid receptor.Cell Metab. 2010 Jun 9;11(6):517-3)* as an alternative model for the work in this aim. Runx2 is expressed earlier in the differentiation of bone cells and would increase the effect of Klotho loss by affecting a greater percentage of bone. This should enhance the effects we have already seen in other lines and enable us to delve further into physiology of the phenotype. We have begun the process to import these mice into our lab. We will then make a decision regarding which of the two lines to use to continue the work in this aim.

Opportunities for Training and Professional Development

Dr. Beate Lanske (Principal Investigator) attended the following conferences
ASBMR CONFERENCE, October 2013:
Dr. Lanske gave a state of the art lecture on *"Pth-Fgf23-Klotho: who is in charge?"* She also acted as a reviewer for a poster session and three year term as ASBMR councilor, where she will also function as the liaison between the ASBMR Council and the Women's Committee.
ASBMR COUNCIL, February 2014:
Dr. Lanske attended the winter ASBMR Council meeting in Washington DC and visited Capitol Hill together with other members of the ASBMR and patients (affected by X-linked hypophosphatemia-XLH, osteoporosis and Osteogenesis imperfect) to speak about her work. Especially interesting was the interaction with XLH patients since the mouse models Dr. Lanske has established during the past 10 years are related to that disease.
GRC, August 2014:
Dr. Lanske attended and spoke at the Gordon Research Conference "Biomineralization", which took place in New London, NH.
Importantly, the meetings she attended provided the opportunity to start and continue new and existing collaborations and discuss areas relevant to this grant with colleagues and peers, including FGF23, Klotho, PTH, calcium/phosphate homeostasis and mineralization.

Dr. Noriko Ide (postdoctoral fellow) and Dr. Junichi Hanai (collaborator)
Drs. Ide and Hanai have been working closely together to analyze the phenotype of *Kapcre;Klotho*$^{fl/fl}$ using various techniques. Dr. Ide has learned a great deal in the techniques FACs sorting and magnetic bead isolation of cells and these have been important for this project. She has been attending a number of local lecture series on related topics.

Hao Wang (Research Assistant)
Mr. Wang has been trained in maintaining a mouse colony and genotyping. He has taken some courses and individual training sessions with my lab manager.

Katsuhiko Amano (postdoctoral fellow)
Dr. Amano has been performing all IHC and histological bone analyses for all three aims. He also has been teaching other postdocs in these procedures.

Hirotake Komaba (postdoctoral fellow)
Dr. Komaba has been setting up the 5/6 nephrectomy protocol for our lab and has now optimizing this technique.

Dr. Jovana Kaludjerovic (postdoctoral fellow)
GRC, March 2014:
Dr. Kaludjerovic attended the Gordon Research Conference "Fibroblast Growth Factors in Development and Disease" in Venture, CA. This provided her a good networking environment.
ENDOCRINE SOCIETY, June 2014:
Dr. Kaludjerovic attended the Career Development Workshop at the ENDO meeting She currently has a postdoctoral fellowship from Canada. She maintains memberships in the American Society for Bone and Mineral Research (ASBMR), American Society for Nutrition (ASN), Canadian Nutrition Society (CNS), The Endocrine Society (ENDO), European Society of Endocrinology (ESE), Young Active Research in Endocrinology (YARE), Graduate Women in Science (GWIS), Canadian Association of Postdoctoral Scholars and Harvard Postdoctoral Association. Dr. Kaludjerovic has mentored a postgraduate student during this year who helped her analyze some of the data in Aim 3. She also mentored in the Advanced Graduate Education Program at Harvard.

Dissemination of Results

The studies for part of Aim 2 and all of Aim 3 are ongoing and results are not ready for publication. We have published the results of our preliminary work and final results for Aim 1 and parts of Aim 2.

Plans for Next Reporting Period

Aim 1 ***PTHCre; Klotho$^{fl/fl}$*** **Mice** completed

Aim 2 ***KSPcre; Klotho$^{fl/fl}$*** **Mice** eliminated

As mentioned in the SOW, we have dropped this line of mice. This is due to a publication on this topic by one of our former collaborators before our funding started. We believe that it is not necessary to duplicate the study.

(Olauson H, Lindberg K, Amin R, Jia T, Wernerson A, Andersson G, Larsson TE. Targeted deletion of Klotho in kidney distal tubule disrupts mineral metabolism. J Am Soc Nephrol. 2012 Oct;23(10):1641-51).

Aim 2 ***Six2cre; Klotho$^{fl/fl}$*** **Mice** completed

Aim 2 ***KAPcre;Klotho$^{fl/fl}$*** **Mice** ongoing & expanded

We are planning to finalize and publish the results on *KAPcre;Tomato $^{fl/fl}$;Klotho$^{fl/fl}$*. Due to some unforeseen complications with the *Kapcre* transgenic mice, which require induction by testosterone for full efficiency, we have been searching for a more appropriate *cre* transgenic mouse line where Cre is strongly expressed in PCTs. Such a mouse has been recently published and we have already obtained this mouse for our laboratory.

We have started generating the new *SLC34a1^{GCE};Tomato $^{fl/fl}$;Klotho$^{fl/fl}$* mice and will perform similar studies as with the original *KAPcre;Tomato $^{fl/fl}$;Klotho$^{fl/fl}$* mouse line. These will be available for first characterization in the first half of the new reporting period. The experiments listed in Task 2 (see Major Goals and Tasks above) will begin as soon as sufficient mice are available. We plan to complete macroscopic and biochemical analyses and routine histology. Quantitative analysis of bone, gene and protein expression studies will be started but not completed during the period.

Aim 3 ***Prx1cre;Klotho$^{fl/fl}$*** **Mice** ongoing

We have started to examine the bones of these mice and are currently waiting for the histomorphometric analyses of mice on control and adenine diet. We are planning to finalize all experiments by adding a few more numbers of mice. We then will start writing one or two manuscripts. If we can confirm all of the exciting findings of this project, the publication will be in a high impact journal.

Aim 3 ***DMP1cre;Klotho$^{fl/fl}$*** **Mice** just started

We recently generated this new mouse strain and have started to perform Sham and 5/6 nephrectomy on these mice. We have also established the in vitro isolation of osteocytes using the tomato reporter for our cell culture experiments. We plan to follow the experimental design as suggested in the SOW and hope to confirm observations made in *Prx1cre;Klotho$^{fl/fl}$* mice and to discover new roles of Klotho since in these mice Klotho will be deleted from all osteocytes throughout the skeleton, in contrast to the selective deletion in limbs and calvaria with Prx1 Cre.

Aim 3 ***Col1(α1)cre;Klotho$^{fl/fl}$*** **Mice** to be started, maybe expanded

We have not started to work on this project yet. Based on the data we have obtained so far from the other two bone specific Klotho deletion mouse models listed in Aim 3, we have been discussing whether we should switch from using these *Col1(α1)cre* to a more recent model, Runx2cre transgenic mice. The advantage of this new Runx2 cre transgenic mouse line would be that the Klotho deletion would take place in a larger pool of osteoblasts.

4. Impact

Nothing to report

5. Changes/Problems

Changes in Approach

1. We incorporated *Tomato $^{fl/fl}$* in some of the transgenic lines. This slightly extended the period for generating the lines but made the characterization of Klotho ablation more efficient (Task 1). The impact on the time for the task was minimal.
2. We will be generating *SLC34a1^{GCE};Tomato $^{fl/fl}$;Klotho$^{fl/fl}$* mice in addition to the *KAPcre;Tomato $^{fl/fl}$;Klotho$^{fl/fl}$* mice for the reasons stated above. This will shift this portion of the project into later stages of the project but the work should be completed within the overall life of the project. Mice will not have to be maintained for a long a period as required by the KAP Cre approach and data can be collected at earlier ages.
3. We are considering *Runx2cre;Tomato$^{fl/fl}$;Klotho$^{fl/fl}$* mice in addition or instead of to the *Col1(α1)*cre mice for reasons stated above.

Problems

We have completed the work on AIM 1 and part of AIM 2, which was published in the past period of funding.

Aim 1: *PTHCre; Klotho$^{fl/fl}$* Mice

This aim was carried out together with a group in Sweden and they have progressed very fast with the analysis during the first few months of this DoD funding. The paper was published in PLOS Genetics. Unfortunately, the report of funding from DoD was somehow omitted and we are very sorry for this mistake.

*Parathyroid-specific deletion of Klotho unravels a novel calcineurin-dependent FGF23 signaling pathway that regulates PTH secretion. Olauson H, Lindberg K, Amin R, Sato T, Jia T, Goetz R, Mohammadi M, Andersson G, **Lanske B**, Larsson TE. PLoS Genet. 2013;9(12):e1003975. Epub 2013 Dec 12.*

Aim 2: *Six2cre; Klotho$^{fl/fl}$* Mice

This aim was partly carried out in my laboratory and partly in the laboratory at the Karolinska Institute. Dr. Larsson has recently published the data on this work, but did not request my funding source before publication. We will make sure that this will not happen anymore.

*The kidney is the principal organ mediating klotho effects. Lindberg K, Amin R, Moe OW, Hu MC, Erben RG, Ostman Wernerson A, **Lanske B**, Olauson H, Larsson TE. J Am Soc Nephrol. 2014 Oct;25(10):2169-75. doi: 10.1681/ASN.2013111209. Epub 2014 May 22.*

Delays and Planned Resolution

We anticipate no significant delays.

Changes Impacting Expenditures

We anticipate no changes.

Changes in Use or Care of Subjects, Biohazards, Agents

There are no changes to report.

6. Products

Two manuscripts have been published during the first year of funding in which Dr. Lanske is listed as second last and third last author

a) *Parathyroid-specific deletion of Klotho unravels a novel calcineurin-dependent FGF23 signaling pathway that regulates PTH secretion. Olauson H, Lindberg K, Amin R, Sato T, Jia T, Goetz R, Mohammadi M, Andersson G,* ***Lanske B****, Larsson TE. PLoS Genet. 2013;9(12):e1003975. Epub 2013 Dec 12.*
b) *The kidney is the principal organ mediating klotho effects. Lindberg K, Amin R, Moe OW, Hu MC, Erben RG, Ostman Wernerson A,* ***Lanske B****, Olauson H, Larsson TE. J Am Soc Nephrol. 2014 Oct;25(10):2169-75. doi: 10.1681/ASN.2013111209. Epub 2014 May 22.*

7. Participants & Other Collaborating Organizations

Individuals Working on Project

The following individuals have participated in the project during the reporting period.

Name	**Beate Lanske, PhD**
Project Role	Principal Investigator
Researcher Identifier	
Nearest Person-Month Worked	2.4
Contribution to Project	Planning of experiments, reviewing data, writing manuscripts
Funding Support	DoD, NIH, HSDM

Name	**Mohammed S Razzaque, MD PhD**
Project Role	other significant contributor
Researcher Identifier	
Nearest Person-Month Worked	0.6
Contribution to Project	discussion of data and interpretation of results, reviewing data,
Funding Support	DoD, NIH, HSDM

Name	**Junichi Hanai, MD PhD**
Project Role	Collaborator
Researcher Identifier	
Nearest Person-Month Worked	0.6
Contribution to Project	Technical support and interpretation of data as nephrologist
Funding Support	DoD, BIDMC

Name	**Noriko Ide, MD PhD**
Project Role	Postdoctoral Fellow
Researcher Identifier	
Nearest Person-Month Worked	12
Contribution to Project	Aim 2 KapCre-Klotho
Funding Support	DoD

Name	**Hao Wang**
Project Role	Research Assistant
Researcher Identifier	
Nearest Person-Month Worked	3
Contribution to Project	Maintenance of mouse lines, genotyping
Funding Support	DoD, NIH

Name	**Katsuhiko Amano, DDS PhD**
Project Role	Postdoctoral Fellow
Researcher Identifier	
Nearest Person-Month Worked	5
Contribution to Project	Histological analysis of bones in all aims
Funding Support	DoD, NIH

Name	**Jovana Kaludjerovic, PhD**
Project Role	Postdoctoral Fellow
Researcher Identifier	
Nearest Person-Month Worked	6
Contribution to Project	Aim 3 Prx1Cre-Klotho
Funding Support	Canadian fellowship

Name	**Hirotaki Komaba, MD PhD**
Project Role	Postdoctoral Fellow
Researcher Identifier	
Nearest Person-Month Worked	3
Contribution to Project	Aim 3 Dmp1Cre-Klotho
Funding Support	Japanese fellowship

Changes in Active Support

Nothing to report.

Other Organizations

Nothing to report.

8. Special Reporting Requirements

Nothing to report

9. Appendices

2 PDF files for published manuscripts.

OPEN ACCESS Freely available online

PLOS | GENETICS

Parathyroid-Specific Deletion of *Klotho* Unravels a Novel Calcineurin-Dependent FGF23 Signaling Pathway That Regulates PTH Secretion

Hannes Olauson[1], Karolina Lindberg[1], Risul Amin[1], Tadatoshi Sato[2], Ting Jia[1], Regina Goetz[3], Moosa Mohammadi[3], Göran Andersson[4], Beate Lanske[2], Tobias E. Larsson[1,5]*

1 Division of Renal Medicine, Department of Clinical Science, Intervention and Technology, Karolinska Institutet, Stockholm, Sweden, **2** Department of Oral Medicine, Infection, and Immunity, Harvard School of Dental Medicine, Boston, Massachusetts, United States of America, **3** Department of Biochemistry and Molecular Pharmacology, New York University School of Medicine, New York, New York, United States of America, **4** Division of Pathology, Department of Laboratory Medicine, Karolinska Institutet and Karolinska University Hospital Huddinge, Stockholm, Sweden, **5** Department of Nephrology, Karolinska University Hospital, Stockholm, Sweden

Abstract

Klotho acts as a co-receptor for and dictates tissue specificity of circulating FGF23. FGF23 inhibits PTH secretion, and reduced Klotho abundance is considered a pathogenic factor in renal secondary hyperparathyroidism. To dissect the role of parathyroid gland resident Klotho in health and disease, we generated mice with a parathyroid-specific *Klotho* deletion (*PTH-KL*$^{-/-}$). *PTH-KL*$^{-/-}$ mice had a normal gross phenotype and survival; normal serum PTH and calcium; unaltered expression of the *PTH* gene in parathyroid tissue; and preserved PTH response and sensitivity to acute changes in serum calcium. Their PTH response to intravenous FGF23 delivery or renal failure did not differ compared to their wild-type littermates despite disrupted FGF23-induced activation of the MAPK/ERK pathway. Importantly, calcineurin-NFAT signaling, defined by increased MCIP1 level and nuclear localization of NFATC2, was constitutively activated in *PTH-KL*$^{-/-}$ mice. Treatment with the calcineurin-inhibitor cyclosporine A abolished FGF23-mediated PTH suppression in *PTH-KL*$^{-/-}$ mice whereas wild-type mice remained responsive. Similar results were observed in thyro-parathyroid explants *ex vivo*. Collectively, we present genetic and functional evidence for a novel, Klotho-independent, calcineurin-mediated FGF23 signaling pathway in parathyroid glands that mediates suppression of PTH. The presence of Klotho-independent FGF23 effects in a Klotho-expressing target organ represents a paradigm shift in the conceptualization of FGF23 endocrine action.

Citation: Olauson H, Lindberg K, Amin R, Sato T, Jia T, et al. (2013) Parathyroid-Specific Deletion of *Klotho* Unravels a Novel Calcineurin-Dependent FGF23 Signaling Pathway That Regulates PTH Secretion. PLoS Genet 9(12): e1003975. doi:10.1371/journal.pgen.1003975

Editor: Thomas O. Carpenter, Yale University, United States of America

Received June 13, 2013; **Accepted** October 9, 2013; **Published** December 12, 2013

Funding: This work was supported by the Swedish Foundation for Strategic Research, Swedish Research Council, Swedish Kidney Foundation, grants from Karolinska Institutet and Karolinska University Hospital, and United States National Institutes of Health grants DE13686 (to MM) and DK073944 and DK097105 (to BL). The funders had no role in study design, data collection and analysis, decision to publish, or preparation of the manuscript.

Competing Interests: The authors have declared that no competing interests exist.

* E-mail: tobias.larsson@ki.se

Introduction

Calcium plays a pivotal role in many biological processes, such as intra-cellular signaling, cell membrane depolarization and excitation, energy metabolism and skeletal mineralization. Accordingly, a fine-tuned regulation of serum calcium level is a prerequisite for normal cellular and organ function in most organisms. Parathyroid hormone (PTH) is the principal hormonal regulator of circulating calcium as it rapidly increases its renal tubular reabsorption and mobilization from bone deposits in response to a decrease in serum calcium [1]. In turn, free calcium ions can efficiently inhibit PTH secretion as part of an endocrine feedback loop mediated by the calcium-sensing receptor (CaSR) located on parathyroid chief cells [2].

Type I membrane-bound alpha-Klotho (Klotho) defines tissue specificity for the phosphaturic hormone fibroblast growth factor-23 (FGF23) by acting as a permissive co-receptor [3]. Klotho is predominantly expressed in organs requiring abundant calcium transport such as kidneys, parathyroid glands and choroid plexus [4]. In the parathyroids, FGF23 binds to binary complexes of an FGF receptor (FGFR) and Klotho to suppress PTH secretion [5,6]. Klotho activity on the other hand has been implicated as fundamental for the stimulation of PTH secretion during hypocalcemic conditions [7], although the underlying mechanism has been challenged [8].

Secondary hyperparathyroidism (sHPT) is a common manifestation in chronic kidney disease (CKD) despite markedly increased serum FGF23 concentrations. This presumably reflects parathyroid resistance to FGF23 action, which was also supported by lack of response to FGF23 injections in a rat model of CKD [9,10]. The proposed mechanism underlying such FGF23 resistance is decreased abundance of parathyroid Klotho and FGFRs [11,12].

To dissect the role of parathyroid gland resident Klotho in physiology and in pathophysiological states such as CKD, we generated a novel mouse strain harboring a parathyroid-specific deletion of the *Klotho* gene. The present study sheds new light on the function of parathyroid Klotho and identifies a novel, Klotho-independent signaling pathway of FGF23 that is involved in the regulation of PTH secretion.

Author Summary

Inorganic calcium is a critical element for a diverse range of cellular processes ranging from cell signaling to energy metabolism, and its extracellular concentration is controlled by parathyroid hormone (PTH). Klotho is expressed in parathyroid chief cells and reported to facilitate PTH secretion during hypocalcemia and mediate FGF23 suppression of PTH synthesis and secretion. To dissect the role of parathyroid Klotho in health and disease, we generated parathyroid-specific *Klotho* knockout mice. The mutant mice had normal serum levels of PTH and calcium. Further, their parathyroid sensitivity to acute fluctuations in serum calcium and response to FGF23 treatment were preserved, and mutant mice developed secondary hyperparathyroidism of similar magnitude as wild-type mice when challenged with renal failure. A previously unknown parathyroid FGF23 signaling pathway involving calcineurin was constitutively activated in the mutant mice, and blocking this pathway abolished FGF23-induced suppression of PTH secretion. Our data challenges the concepts of Klotho as a mandatory factor for the acute hypocalcemic PTH response and decreased Klotho abundance as a pathogenic factor in secondary hyperparathyroidism. Finally, the presence of Klotho-independent FGF23 effects in a Klotho-expressing target organ represents a paradigm shift in the conceptualization of FGF23 endocrine action.

Results

Generation of *PTH-KL*$^{-/-}$ mice

Mice with a parathyroid specific deletion of Klotho (*PTH-KL*$^{-/-}$) were generated using Cre-LoxP recombination (Figure S1). Floxed Klotho mice were crossed with mice expressing Cre recombinase driven by the human PTH promoter, which was previously shown to have Cre activity exclusively in the parathyroid glands [13]. Successful deletion of parathyroid Klotho protein was confirmed with immunohistochemical staining of thyro-parathyroid tissue (Figure 1). Overall efficiency of deletion varied, and was up to >90% in investigated samples. Subanalyses of mice with the most efficient deletion showed similar results to the full analyses.

Gross phenotype and survival of *PTH-KL*$^{-/-}$ mice

Adult *PTH-KL*$^{-/-}$ mice were viable, fertile and did not display any gross physical or behavioral abnormalities. Survival was similar to wild-type littermates during the study with no mortality up to 6 months of age. Female *PTH-KL*$^{-/-}$ mice had reduced body weight and crown-rump length compared to wild-type littermates ($p<0.05$; Figure 1), whereas no such differences were found in male *PTH-KL*$^{-/-}$ mice.

Serum and urine biochemistries of *PTH-KL*$^{-/-}$ mice

Serum biochemistries in 8-week-old mice are shown in Figure 1. Interestingly, the serum levels of 1,25-dihydroxy vitamin D_3 ($1,25(OH)_2D$) were doubled in *PTH-KL*$^{-/-}$ mice compared to their wild-type littermates ($p<0.05$), while PTH, calcium and FGF23 remained normal. Serum phosphorous (wild-type vs *PTH-KL*$^{-/-}$; 9.54 ± 0.38 vs 9.39 ± 0.32, $p>0.05$), creatinine (0.31 ± 0.03 vs 0.26 ± 0.02, $p>0.05$), urinary concentrations of calcium/creatinine (0.53 ± 0.19 vs 0.53 ± 0.19, $p>0.05$) and phosphorous/creatinine (19.1 ± 3.4 vs 19.4 ± 3.0, $p>0.05$) were also unaltered in *PTH-KL*$^{-/-}$ mice. To exclude the possibility of early onset changes in mineral metabolism, we analyzed serum from 3-week-old animals. No differences were seen for serum calcium (wild-type vs *PTH-KL*$^{-/-}$; 10.00 ± 0.22 vs 9.86 ± 0.20, $p>0.05$) or PTH (118.0 ± 13.4 vs 133.0 ± 21.8, $p>0.05$).

Bone and renal phenotype of *PTH-KL*$^{-/-}$ mice

We investigated potential secondary effects that the parathyroid-specific deletion of the *Klotho* gene might have on the main target organs of PTH signaling, namely bone and kidney. There were no significant histological changes in bone from 6-week old *PTH-KL*$^{-/-}$ mice and bone mineral density was unaltered compared to wild-type mice (Figure S2). Renal histology was also normal and no transcriptional changes were found for *Klotho*, *VDR*, *Cyp27b1*, *Cyp24a1*, *Npt2a*, *TRPV5* or *CaSR* in kidneys from *PTH-KL*$^{-/-}$ mice compared to wild-type mice (Table S1).

Parathyroid histology and protein expression in *PTH-KL*$^{-/-}$ mice

Parathyroid size, histology and proliferation index, defined as Ki67 positive cells/total number of cells, was not affected by the *Klotho* gene deletion (wild-type vs *PTH-KL*$^{-/-}$, 2.9% vs. 2.8%, $p>0.05$) (Figure S3A). Immunofluorescence staining showed no significant changes in protein expression for PTH, CaSR, VDR (Figure S3B), FGFR1 or Cyp27b1 (data not shown) suggesting that Klotho does not regulate the expression of these proteins in an autocrine or paracrine fashion under physiological conditions.

Expression of genes critical for parathyroid function in *PTH-KL*$^{-/-}$ mice

The expression of approximately 90 genes critical for parathyroid function was examined using a nanostring array. The data are compiled in Table S2. In addition to *Klotho*, changes in expression level were observed for genes important for transcriptional and metabolic control, such as *Cfd* (Entrez Gene: 11537), *Fabp4* (11770) and *Smad4* (17128)(Figure 2). *Gli3* (14634), *Pin1* (23988), *sFRP3* (20379) and *FGF20* (80857) were also expressed at different levels in the parathyroids of *PTH-KL*$^{-/-}$ mice compared to wild-type mice, although at a low absolute level. Notably, the expression of some of the genes that play a key role in the function of the parathyroid gland, such as *PTH*, *Gata3*, *CaSR* and *VDR*, or in FGF23 physiology, such as *FGFR1* and the vitamin D regulatory enzymes *Cyp27b1* and *Cyp24a1*, were not significantly affected by the knockdown of parathyroid *Klotho* gene expression.

Parathyroid sensitivity and response to rapid changes in serum calcium in *PTH-KL*$^{-/-}$ mice

The serum calcium level of *PTH-KL*$^{-/-}$ and wild-type mice was either rapidly decreased or increased by an intraperitoneal injection of EGTA or calcium-gluconate, respectively [14]. The parathyroid response to alterations in serum calcium, as measured by serum PTH level, did not differ between *PTH-KL*$^{-/-}$ mice and wild-type mice (wild-type vs *PTH-KL*$^{-/-}$, $R^2=0.77$, $p<0.0001$ vs $R^2=0.74$, $p<0.0001$)(Figure S4), supporting that parathyroid Klotho is not essential for parathyroid sensitivity to acute changes in serum calcium, and its response to them with altered PTH secretion.

Parathyroid response to induction of renal failure in *PTH-KL*$^{-/-}$ mice

Renal insufficiency is associated with the development of sHPT. To test whether parathyroid function is different in *PTH-KL*$^{-/-}$ mice under conditions of renal insufficiency, we induced renal failure using an adenine-based protocol [15]. Four weeks after induction of renal insufficiency, *PTH-KL*$^{-/-}$ mice exhibited sHPT

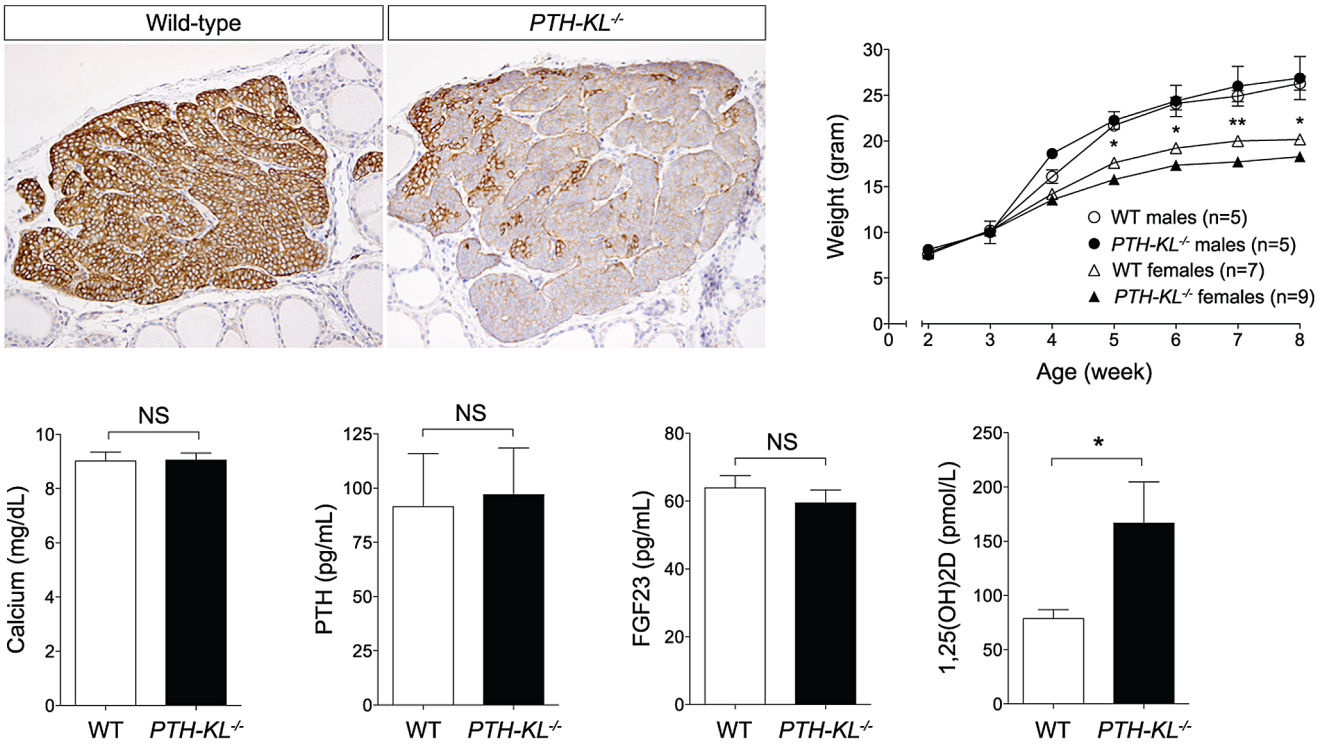

Figure 1. Tissue-specific deletion of the *Klotho* gene. *Upper left panel*. Immunohistochemical staining confirmed successful deletion of Klotho in parathyroid glands of *PTH-KL*$^{-/-}$ mice. 20× magnification. *Upper right panel*. The gross appearance of *PTH-KL*$^{-/-}$ mice was normal although females had lower body weight and shorter crown-rump length compared to wild-type littermates. No differences were seen for male *PTH-KL*$^{-/-}$ mice. *p<0.05 **<0.01. *Lower panel:* Serum levels of 1,25(OH)$_2$D were doubled in *PTH-KL*$^{-/-}$ mice compared to their wild-type littermates (p<0.05), while PTH, calcium and FGF23 remained normal.
doi:10.1371/journal.pgen.1003975.g001

just like their wild-type littermates did. Its severity as well as changes in other markers of mineral metabolism was similar among *PTH-KL*$^{-/-}$ and wild-type mice (Figure 3A and Table S3). Notably, serum FGF23 levels were increased by approximately 50-fold in both *PTH-KL*$^{-/-}$ and wild-type mice with renal failure compared to mice with preserved renal function.

Parathyroid response to FGF23 in *PTH-KL*$^{-/-}$ mice

Based on our findings that the parathyroid glands of *PTH-KL*$^{-/-}$ mice retained calcium sensitivity and that sHPT developed similarly as in wild-type mice upon induction of renal insufficiency, we reasoned that the parathyroid response to FGF23 might also be preserved in *PTH-KL*$^{-/-}$ mice. To test this, we injected mice intravenously with a single dose of recombinant FGF23 and measured serum concentrations of PTH before and 15 min after the injection. As shown in Figure 3B, FGF23 caused a decrease in serum levels of PTH in *PTH-KL*$^{-/-}$ mice of similar magnitude as in wild-type mice.

FGF23 signaling pathway in the parathyroid glands of *PTH-KL*$^{-/-}$ mice

We next explored which signaling pathway might mediate the inhibition by FGF23 on PTH secretion in *PTH-KL*$^{-/-}$ mice. Activation of the MAPK cascade was first examined using immunofluorescence staining. As shown in Figure 3C, there was significantly less immunostaining for phosphorylated ERK1/2 in parathyroid tissue from *PTH-KL*$^{-/-}$ mice, and a complete co-localization with residual Klotho protein. These data indicate that activation of the MAP kinase pathway by FGF23 is markedly suppressed or absent in Klotho-deficient parathyroids.

We next tested whether the calcineurin-nuclear factor of activated T cells (NFAT) pathway, another proposed downstream signaling pathway of FGFR activation [16,17,18], was activated in the parathyroids of *PTH-KL*$^{-/-}$ mice in response to FGF23. To this end, we analyzed gene expression of calcineurin and NFAT in parathyroid tissue from wild-type mice. Indeed, all subunits of

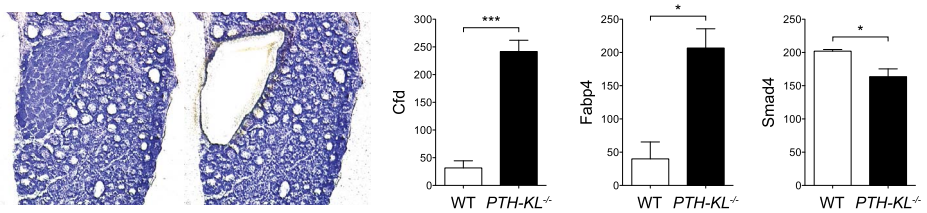

Figure 2. Parathyroid transcriptional data. Transcriptional analysis of laser microdissected parathyroid tissue revealed differential expression of *Cfd*, *Smad4* and *Fabp4* in *PTH-KL*$^{-/-}$ mice (n = 3 for each genotype). *p<0.05 ***p<0.001.
doi:10.1371/journal.pgen.1003975.g002

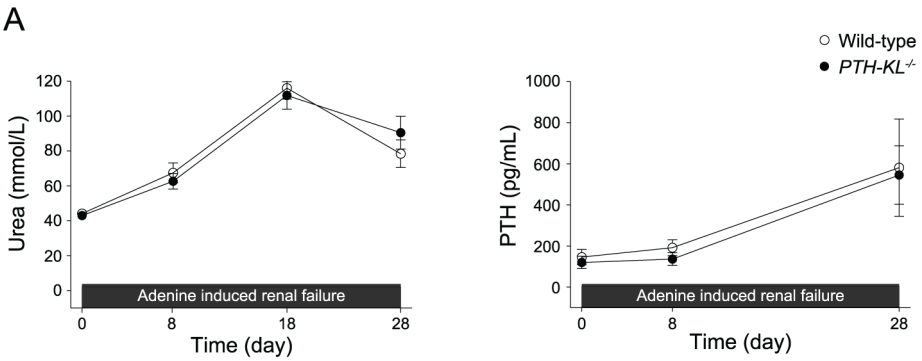
A
Urea (mmol/L)
120
100
80
60
40
20
0
Adenine induced renal failure
0
8
18
28
Time (day)
Wild-type
PTH-KL-/-
PTH (pg/mL)
1000
800
600
400
200
0
Adenine induced renal failure
0
8
28
Time (day)

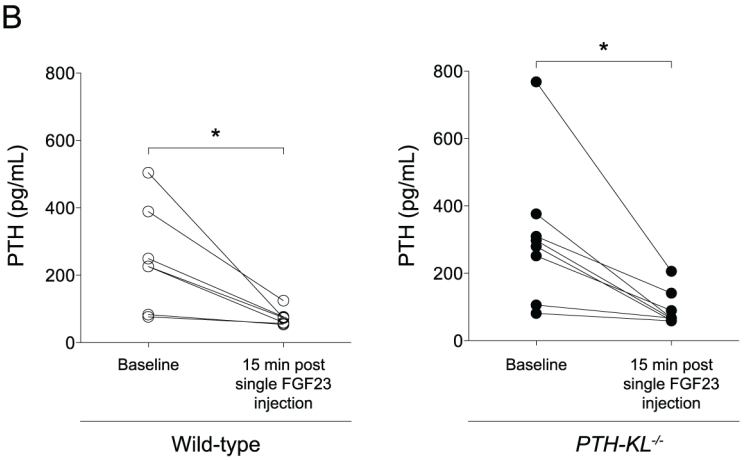
B
PTH (pg/mL)
800
600
400
200
0
*
Baseline
15 min post single FGF23 injection
Wild-type
PTH (pg/mL)
800
600
400
200
0
*
Baseline
15 min post single FGF23 injection
PTH-KL-/-

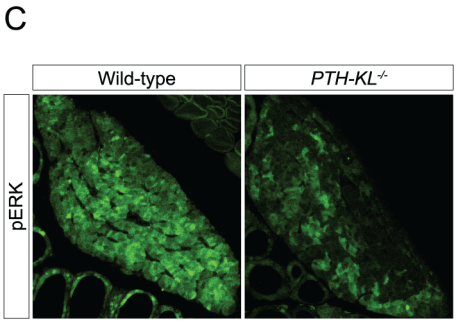
C
Wild-type
PTH-KL-/-
pERK

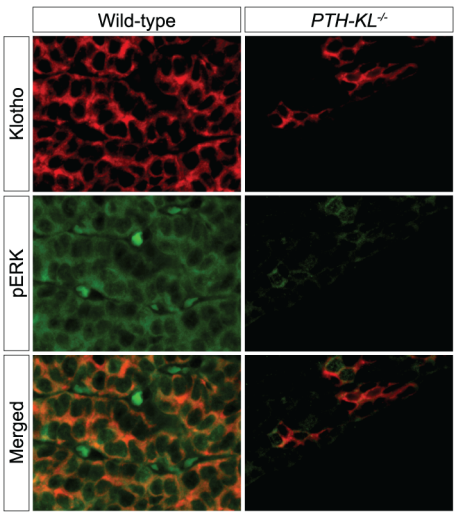
Wild-type
PTH-KL-/-
Klotho
pERK
Merged

Figure 3. Responsiveness to renal failure and a single FGF23 injection. A) Mice were challenged with renal failure during 4 weeks by dietary adenine delivery. *PTH-KL*$^{-/-}$ (n = 8) and wild-type (n = 6) mice developed uremia and secondary hyperparathyroidism of similar magnitude. B) Mice were injected intravenously with recombinant FGF23 protein at the dose 0.15 mg/kg and blood samples from the tail vein were drawn after 15 minutes. *PTH-KL*$^{-/-}$ mice had a similar rapid reduction in PTH followed by a single FGF23 injection indicating a preserved FGF23 responsiveness in *PTH-KL*$^{-/-}$ mice despite ablated Klotho expression. Figure shows pooled data from two independent experiments (n = 9 for *PTH-KL*$^{-/-}$; n = 7 for wild-type mice). *$p<0.05$ C) The impact of Klotho-dependent FGF23 signaling was investigated in parathyroid glands with dual immunofluorescence staining of Klotho and phosphorylated ERK1/2. Importantly, phosphorylated ERK1/2 was strongly induced 15 minutes after a single intravenous FGF23 injection in wild-type mice. In contrast, *PTH-KL*$^{-/-}$ mice failed to phosphorylate ERK1/2 specifically in cells lacking Klotho, supporting a disruption of functional Klotho-mediated FGF23 signaling in *PTH-KL*$^{-/-}$ mice (10× and 40× magnification).
doi:10.1371/journal.pgen.1003975.g003

calcineurin and all four calcium-regulated members of the NFAT family (NFATC1–NFATC4) were expressed in the parathyroid of wild-type mice (Figure 4A). We then examined by immunofluorescence microscopy the subcellular distribution of the NFAT proteins in parathyroid tissue from *PTH-KL*$^{-/-}$ mice that had been treated with FGF23. While parathyroid tissue from FGF23 treated wild-type mice showed cytoplasmic immunostaining for NFATC2, the parathyroid tissue of FGF23 treated *PTH-KL*$^{-/-}$ mice also showed nuclear localization of NFATC2 (Figure 4B). No clear difference was seen for the other NFATs. In addition, immunostaining analysis for the modulatory calcineurin interacting protein 1 (MCIP1), a facilitator of calcineurin activity, revealed that MCIP1 expression was markedly upregulated in Klotho-deficient parathyroid tissue compared to wild-type tissue (Figure 4B) [19]. Together, the data suggest that the calcineurin-NFAT pathway is activated in the parathyroid of *PTH-KL*$^{-/-}$ mice, and responds to treatment with FGF23.

To provide *in vivo* evidence for the role of the calcineurin-NFAT pathway in mediating the suppression by FGF23 of PTH secretion, *PTH-KL*$^{-/-}$ and wild-type mice were pre-treated with cyclosporine A (CsA), a calcineurin-inhibitor, prior to injection of FGF23. As shown in Figures 4C and D, the CsA pre-treatment nearly abolished the effect of FGF23 on PTH secretion in *PTH-KL*$^{-/-}$ mice, whereas it did not impact this FGF23 action in wild-type mice.

To investigate whether the parathyroid calcineurin-NFAT pathway acts independent of serum factors such as soluble Klotho, thyro-parathyroid explants from wild-type and *PTH-KL*$^{-/-}$ mice were treated with FGF23 with or without pre-treatment of CsA [20]. In explants without pretreatment of CsA, 2 h treatment with FGF23 (10 ng/mL) decreased PTH secretion similarly in wild-type and *PTH-KL*$^{-/-}$ mice (Figure 4E). Conversely, in explants pre-treated with CsA (0.83 μM) for 2 h the response to FGF23 treatment was unaltered in wild-type mice but completely blunted in *PTH-KL*$^{-/-}$ mice (ΔPTH relative to baseline; 0.81 vs 1.17, $p<0.01$).

Discussion

Regulation of PTH secretion is a fundamental process in calcium homeostasis, yet our current models are constantly revised due to the complex and multi-dimensional control of PTH. Recent data suggest that, in addition to calcium-sensing receptor and vitamin D receptor activation, the FGF23-Klotho endocrine axis negatively regulates PTH secretion. However, previous discordant results of FGF23-Klotho function in physiology and in pathophysiological states such as renal sHPT prompted us to further investigate the concerted parathyroid action of FGF23-Klotho *in vivo*. We addressed this issue by generating a novel mouse model harboring a parathyroid-specific deletion of *Klotho* and our principal findings are that i) absence of parathyroid Klotho does not alter the acute parathyroid response of PTH secretion and calcium sensitivity as previously suggested; ii) absence of parathyroid Klotho alone does not contribute to the development of renal sHPT; iii) in the absence of parathyroid Klotho, the calcineurin-NFAT pathway is constitutively active and mediates the suppression by FGF23 of PTH secretion. The activation of this compensatory mechanism in Klotho-deficient parathyroids might explain the lack of a hyperparathyroid phenotype in *PTH-KL*$^{-/-}$ mice.

We postulated the existence of a Klotho-independent signaling pathway of FGF23 in the parathyroids based on the findings that *PTH-KL*$^{-/-}$ mice had unaltered serum PTH levels, a intact parathyroid response to FGF23 injections and that hyperparathyroidism was not aggravated in the setting of renal failure despite an effective ablation of parathyroid Klotho and an apparent lack of MAPK activation in response to FGF23. Because FGF23 was recently shown to promote pathological growth of the myocardium and proposed as a mediator of left ventricular hypertrophy through calcineurin-dependent mechanisms [16], we speculated that this pathway might also be activated by FGF23 in the parathyroids. Indeed, there was a marked upregulation of the calcineurin-modulator MCIP1 and a more prominent nuclear localization of NFATC2 in *PTH-KL*$^{-/-}$ mice treated with FGF23, strongly supporting a compensatory activation of the calcineurin-NFAT pathway. The functional importance of this pathway was confirmed *in vivo* and *ex vivo* where pretreatment with the calcineurin inhibitor CsA abolished the PTH response to FGF23 treatment in *PTH-KL*$^{-/-}$ mice but not in wild-type mice. Importantly, our data are also consistent with a previous report demonstrating increased PTH transcript levels in calcineurin Aβ *null* mice and posttranslational regulation of PTH *in vitro* by CsA [21]. The blunted PTH response to FGF23 injection in *PTH-KL*$^{-/-}$ mice indicates that parathyroid FGF23 signaling is dependent on two principal pathways, Klotho-FGFR activation and calcineurin activation respectively. However, the exact intra-cellular mechanisms mediating FGF23 suppression of PTH remain to be defined. Importantly, the expression of FGFR1, which has been implicated as the relevant FGFR for parathyroid FGF23 signaling, was unaltered in *PTH-KL*$^{-/-}$ mice. This supports that their FGF23-driven calcineurin activation occurs without a compensatory increase in its target FGFR.

The identification of a novel FGF23-calcineurin signaling pathway in the parathyroid glands has several implications. First, it challenges the current concepts of FGF23-mediated PTH regulation and secretion. Second, it raises the possibility of previously neglected Klotho-independent down-stream effects of FGF23. This should be put in the context that abnormally high levels of FGF23 in humans are associated with adverse clinical outcomes including cardiovascular disease, CKD progression rate and mortality [22,23,24,25,26,27,28]. Indeed, FGF23 may contribute to pathological left ventricular hypertrophy in a Klotho-independent manner [16]. Future studies are warranted to explore Klotho-independent FGF23 signaling at the systemic level.

Although FGF23 appears to signal independently of Klotho in both parathyroid glands and cardiomyocytes [16] there is a fundamental difference in its signaling in these tissues. In the heart, FGF23 signaling is an 'off-target' effect in a non-classical,

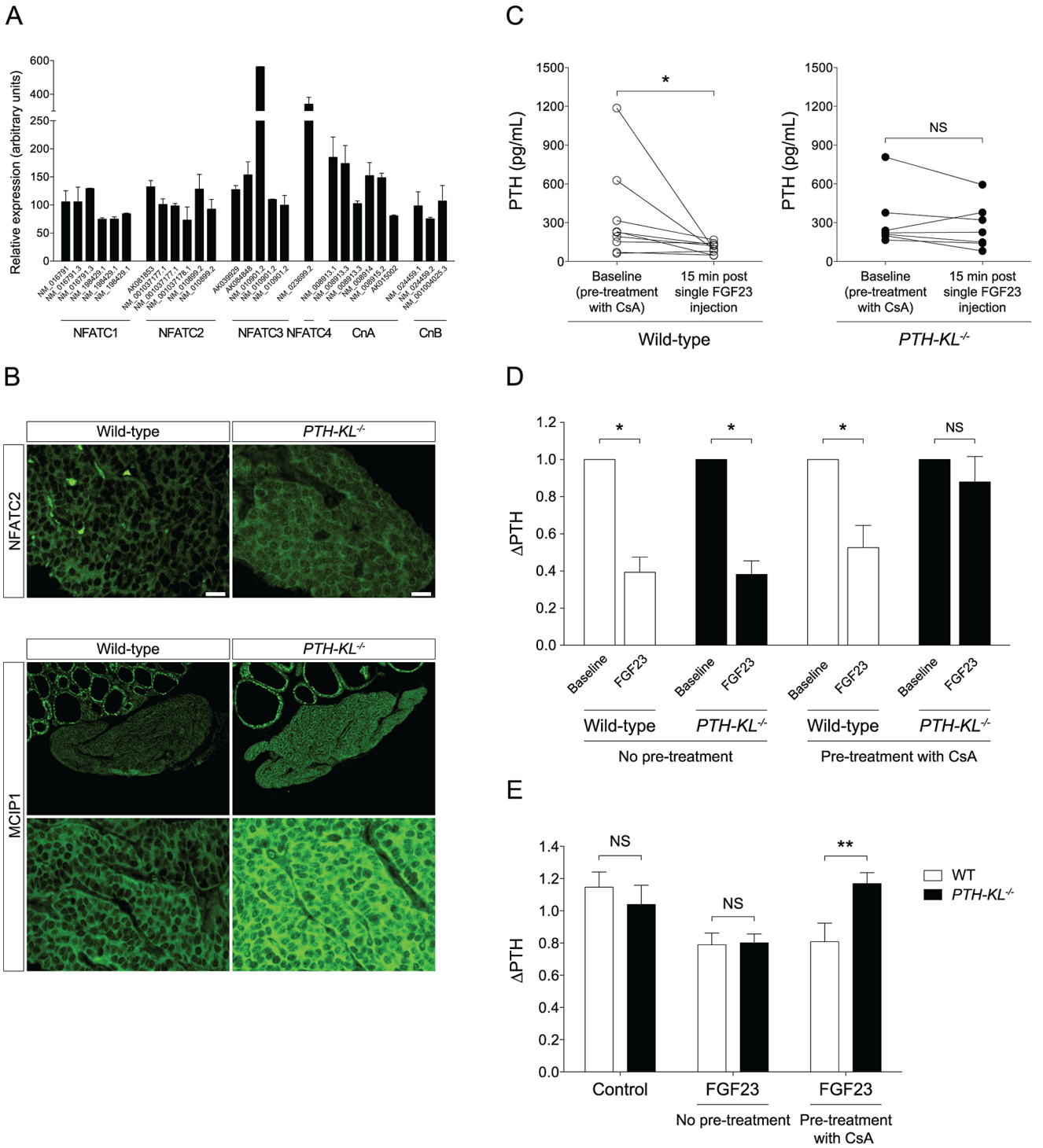

Figure 4. Presence of the calcineurin-NFAT pathway and the impact of cyclosporin A on FGF23 treatment. A) Transcript analysis of laser capture microdissected parathyroid glands from 3- week-old wild-type mice revealed presence of NFATC1-4 and the subunits for calcineurin A and B (CnA and CnB). Each bar represents one hybridization probe. Data is presented as mean (± SEM). B) Immunostaining for NFATC2 showed a partial nuclear translocation in *PTH-KL*$^{-/-}$ mice, and cytoplasmatic localization in wild-type mice after treatment with FGF23, indicating activation of the calcineurin-NFAT pathway in parathyroids of *PTH-KL*$^{-/-}$ mice. In addition, MCIP1, a facilitator of calcineurin signaling, was markedly higher in *PTH-KL*$^{-/-}$ compared to wild-type mice after treatment with FGF23 (10× and 40× magnification). C) Pretreatment of mice with the calcineurin inhibitor CsA followed by a single intravenous FGF23 injection. Wild-type mice had a preserved responsiveness to FGF23 as evidenced by a significant reduction in serum PTH 15 minutes after FGF23 injection ($p<0.05$) whereas FGF23-mediated inhibition of serum PTH was blunted in *PTH-KL*$^{-/-}$ mice. Figure depicts pooled data from two independent experiments, using 60 mg/kg and 150 mg/kg CsA respectively, with similar results. Total n = 10 for wild-type and 7 for *PTH-KL*$^{-/-}$ mice. *$p<0.05$. D) Relative change in PTH level in wild-type and *PTH-KL*$^{-/-}$ mice 15 min after a single FGF23 injection, with and without pretreatment of CsA. E) Thyro-parathyroid explants were cultured in serum-free medium and exposed to FGF23 for 2 h with or without pre-treatment by CsA. Wild-type and *PTH-KL*$^{-/-}$ mice responded with a similar decrease in PTH when exposed to FGF23. In contrast, in

explants pre-treated with CsA (0.83 μM) for 2 h the response to FGF23 treatment was unaltered in wild-type mice but completely blunted in *PTH-KL*$^{-/-}$ mice. N = 5–10 for all groups. **p<0.01.
doi:10.1371/journal.pgen.1003975.g004

non-Klotho expressing organ. In contrast, in parathyroid glands it may rather be viewed as an 'on-target' effect in a Klotho-expressing target organ which represents a paradigm shift in the conceptual framework of FGF23 endocrine action.

SHPT is an inevitable complication in CKD patients with advanced renal failure. Serum FGF23 concentrations rise in parallel with a decline in glomerular filtration rate and are markedly elevated at later stages of CKD [29]. Because PTH stimulates FGF23 synthesis in bone and FGF23 signals back to the parathyroids and suppresses PTH secretion [30], a reasonable assumption is that FGF23 rises in CKD in part to counteract sHPT. Indeed, rats subjected to parathyroidectomy prior to induction of renal failure did not respond with increased FGF23 levels [30]. However, the unabated development of sHPT in the face of extreme FGF23 elevations poses a dilemma: either the inhibitory action of FGF23 on PTH is not relevant *in vivo* or the parathyroids may lack responsiveness to FGF23 in CKD. The latter option is supported by studies in CKD rat models demonstrating an attenuated or abolished parathyroid response to FGF23 [9,10]. Parathyroid FGF23 resistance corroborates data showing a reduction in both Klotho and FGFRs in animal models and in human-derived surgically resected hyperplastic parathyroid glands [11,12]. Our data unequivocally support that parathyroid FGF23 resistance is not primarily induced by Klotho insufficiency. Speculatively, reduced expression of the cognate FGFR(s) could be the principal mechanism underlying this phenomenon.

Another potentially relevant implication of our findings is that a large portion of CKD patients receiving a renal allograft suffer from persistent sHPT unproportional to their residual kidney function in the face of high systemic FGF23 [31]. We speculate that this might be due to a dual blocking of FGF23 signaling, both through the endogenously decreased abundance of parathyroid FGFRs/Klotho and the superimposed inhibition of the calcineurin-NFAT pathway by calcineurin inhibitors (e.g. cyclosporine and tacrolimus) commonly used as immunosuppressive agents. This hypothesis and the proposed role of parathyroid resident Klotho is modeled in Figure 5.

The role of parathyroid Klotho remains controversial due to previous conflicting data. Klotho was reported to modulate parathyroid Na^+/K^+-ATPase activity via direct interaction with its α1-subunit causing an increased abundance of plasma membrane Na^+/K^+-ATPase, which in turn promotes PTH secretion through an increased electrochemical gradient [7]. However, this mechanism was only functional at low extra-cellular calcium concentrations and another study demonstrated that blocking of the Na^+/K^+-ATPase with the digitalis glycoside ouabain did not affect the PTH secretory response to acute hypocalcemia [8]. This study underscores that parathyroid Klotho does not alter parathyroid sensitivity to acute fluctuations in serum calcium.

Given the apparent normal phenotype of *PTH-KL*$^{-/-}$ mice and their intact response to FGF23 it remains uncertain what other functions parathyroid Klotho may have. The cause of increased serum $1,25(OH)_2D$ in *PTH-KL*$^{-/-}$ mice is unknown since expression levels of *Cyp27b1* and *Cyp24a1* are unaltered in kidneys and parathyroid glands. Yet, it is conceivable that parathyroid Klotho has a functional impact on vitamin D metabolism in *PTH-KL*$^{-/-}$ mice and that their elevated $1,25(OH)_2D$ level contributes

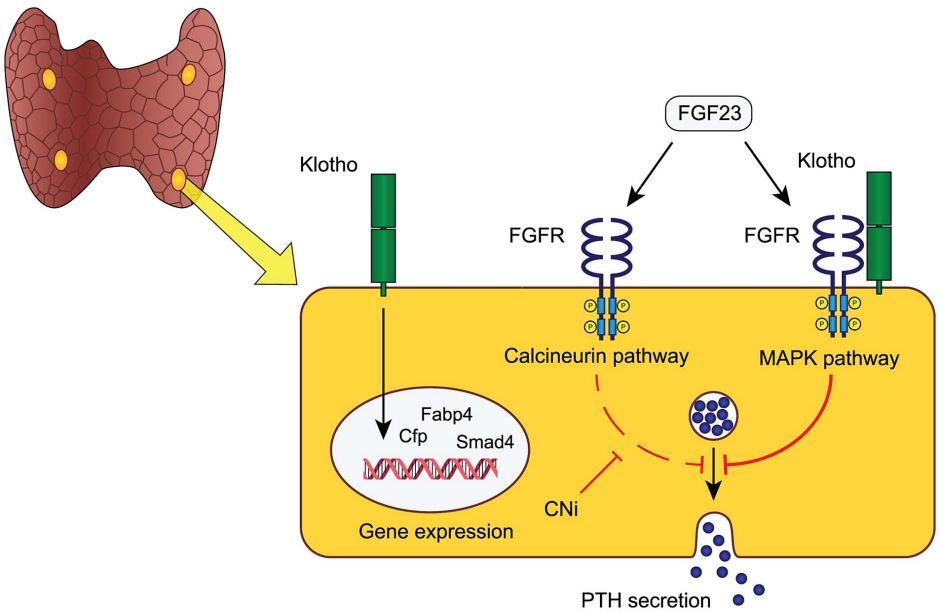

Figure 5. Proposed model of FGF23-Klotho function in parathyroid glands. FGF23 is an endocrine ligand that in the parathyroid glands either binds to an FGF-receptor and membrane-bound Klotho, to elicit activation of the MAPK-pathway, or acts via a calcineurin-dependent signaling pathway. Both pathways induce a rapid inhibition of PTH secretion within 15 minutes. The MAPK-pathway is likely the dominant pathway in physiology, although their relative contributions are unknown. In addition to mediating MAPK-dependent FGF23 signaling, Klotho may play an intrinsic role in modulating parathyroid transcriptional activity for sustained demands and long-term parathyroid function. Speculatively, the clinical use of calcineurin inhibitors (CNi) that block calcineurin signaling may increase the susceptibility to develop, or aggravate pre-existing, hyperparathyroidism in patients with reduced Klotho level such as in chronic kidney disease and primary hyperparathyroidism.
doi:10.1371/journal.pgen.1003975.g005

to normalizing PTH and counteracts development of hyperparathyroidism. Further, we speculate that Klotho is an important local transcriptional regulator of genes involved in sustained challenge of parathyroid function or having a long-term impact on parathyroid function. In support of this idea, *PTH-KL*$^{-/-}$ mice had altered transcript levels of several transcriptional regulators including *Cfd*, *Smad4*, *Fabp4* and *Pin1*. The increased level of *Pin1* in *PTH-KL*$^{-/-}$ mice is intriguing given its role in destabilizing PTH mRNA [32] and may represent yet another protective intracellular mechanism against hyperparathyroidism when FGF23-Klotho signaling is chronically disrupted.

In sum, we dissected the physiological and pathophysiological role of parathyroid Klotho and elucidated several critical and novel aspects in this regard. Most importantly, our study uncovered a Klotho-independent FGF23 signaling mechanism in parathyroid glands with potential implications for multiple disorders of mineral metabolism, especially in CKD.

Materials and Methods

Generation of parathyroid-specific Klotho knockout mice

Mice with a parathyroid-specific Klotho deletion were generated using Cre-Lox recombination as previously described [33]. Briefly, loxP sequences were introduced in the flanking regions of exon 2 of the Klotho gene. Floxed mice were crossed with mice expressing Cre recombinase under the human PTH promotor (129;FVB-Tg(PTH-cre)4167Slib/J; Jackson laboratory, US) and the offspring subsequently analyzed. Floxed littermates not expressing Cre were used as wild-type controls.

Genotyping

Total DNA was extracted from tail biopsies and genotyping performed with standard PCR techniques.

Animal housing

Mice were fed a standard chow (RM1, SDS, UK) containing 0.73% calcium and 0.52% phosphorous. All animals had free access to food and drinking water. Blood sampling was performed by tail vein incision at intermediate time points and through the axillary artery at sacrifice. Animals were fasted 4 hour prior to blood sampling. All experiments were conducted in compliance with the guidelines of animal experiments at Karolinska Institutet and approved by the regional ethical board (Stockholm South ethical committee).

Serum and urine biochemistries

Calcium, phosphorous and creatinine were measured using quantitative colorimetric assay kits (BioChain, US). Urine values were multiplied by 1000. Serum PTH was measured using a Mouse Intact PTH ELISA kit (Immutopics, US). For the FGF23 injection experiments the newer Mouse 1–84 PTH ELISA kit (Immutopics) and plasma samples were used. Serum 1,25-dihydroxy vitamin D was measured using a RIA kit (IDS, US). Intact FGF23 was measured using an FGF23 ELISA kit (Kainos Laboratories, Japan).

RNA isolation and transcript analysis

Parathyroid glands and surrounding adhesive thyroid tissue were carefully removed in conjunction with sacrifice and immediately frozen in OCT. The parathyroid tissue was then dissected using laser capture microdissection. Thirty µm thick cryo-sections were cut and mounted on PEN foil–coated slides (Leica, Germany). Sections were stained with the Arcturus histogene kit (Applied Biosystems, US) and microdissected with a Leica ASLMD microscope (Leica). Total RNA was extracted by the Arcturus picopure RNA isolation kit (Applied Biosystems). The nanostring nCounter system (Nanostring technologies, US) was used to obtain mRNA expression profiles. Data were processed using several normalization strategies, including quantile normalization and 6 house-keeping genes.

Immunohistochemistry and immunofluorescence

Thyro-parathyroid tissue were dissected, fixed in 4% paraformaldehyde and embedded in paraffin. 4 µm sections were immersed in 3% H_2O_2 in methanol, treated with 4% normal serum and blocked with Avidin and Biotin (Vector Laboratories, US). Sections were incubated with primary antibodies at 4°C overnight. For immunohistochemistry slides were incubated with biotinylated secondary antibodies followed by Vector ABC Reagent and developed with DAB substrate (Vector Laboratories). For immunofluorescence, Alexa Fluor conjugated secondary antibodies were used for visualization (Invitrogen, US). The primary antibodies used were rat monoclonal anti-Klotho (KM2076, TransGenic Inc. Japan) mouse monoclonal anti-CaSR (NB120-19347, Novus Biologicals, US), mouse monoclonal anti-VDR (sc-13133, Santa Cruz Biotechnology, US), rabbit monoclonal anti-Ki67 (SP6, Thermo Scientific, US), rabbit monoclonal anti-Erk1/2 and anti-phospho-Erk1/2 (Cell Signaling, US), mouse monoclonal anti-NFATc2 (sc-7295, Santa Cruz Biotechnology) and rabbit polyclonal anti-MCIP1 (a kind gift from Dr. Christian Faul) [34].

Bone phenotyping

Processing of undecalcified bone specimens and cancellous bone histology in the distal femoral metaphysis were performed according to standard protocols. The area within 0.25 mm from the growth plate was excluded from the measurements. µCT were performed using a Scanco Medical µCT 35 system (Scanco, Switzerland).

Determination of parathyroid calcium sensitivity

Investigation of the PTH-calcium relationship was performed by intraperitoneal injections with calcium-gluconate (300 µmol/kg) or EGTA (450 µmol/kg) dissolved in sterile saline as described elsewhere [14]. Blood samples were collected from tail vein for serum PTH and calcium measurements after 30 minutes.

Induction of renal failure

We employed an adenine-based model of renal failure in which mice were given adenine mixed in a casein containing diet. Mice were exposed to 0.3% adenine during the first 7 days followed by 0.2% adenine for 11 days, and finally 0.1% adenine for the rest of the study. Adenine was purchased from Sigma-Aldrich (US), and the powdered casein-based diet from Special Diets Services.

Intravenous injections of FGF23 and pretreatment with CsA

Recombinant human FGF23 protein (A28 to I251) was produced as previously described [35,36]. In all experiments, FGF23 was injected intravenously through the tail vein after a 4-hour fasting period at the dose 0.15 mg/kg dissolved in 300 µl saline. Blood samples were drawn 15 min after injection of FGF23, and the animals were then sacrificed and thyro-parathyroid tissue immediately excised and fixed in 4% formalin for further analysis. Mice were gavage fed with CsA at the dose 60–150 mg/kg (Sigma-Aldrich) two hours prior to FGF23 injection.

Organ culture

During anesthesia the trachea was severed superiorly and inferiorly to the thyroid gland. The trachea-thyro-parathyroid complex was excised and placed in 1 ml serum-free medium (DMEM/F-12, HEPES supplemented with insulin, transferrin and BSA) as previously described [20]. Medium was replaced daily for 4 days before the experiment started, in accordance with the protocol by Ritter et al. On day 4 fresh medium was added and the tissue incubated for 2 h (= baseline). The medium was then replaced with regular medium (= control) or medium containing 10 ng/mL FGF23 and incubated for 2 h. One group was pre-treated with medium containing CsA (0.83 μM) for 2 h prior to incubation with FGF23. All values were calculated as relative change compared to baseline.

Statistical analysis

GraphPad Prism 5.0 (GraphPad Software Inc, US) was used for statistical analysis. Variables were tested with either two-tailed t-test or Mann-Whitney test. Correlations between serum PTH and calcium levels were tested with linear regression analysis.

Supporting Information

Figure S1 Tissue-specific deletion of the *Klotho* gene. *Left panel.* LoxP sites were inserted into intron 1 and 2 of Klotho, enabling targeted disruption of the gene function. Klotho deletion was restricted to parathyroid glands by using transgenic mice expressing Cre recombinase driven by the *PTH* gene promoter. *Right panel.* Representative genotyping by PCR to confirm presence of floxed Klotho alleles.
(PDF)

Figure S2 Bone phenotype of 6 week-old wild-type and *PTH-KL*$^{-/-}$ mice. There were no significant changes in bone mineral density or skeletal histology in *PTH-KL*$^{-/-}$ mice compared to wild-type mice. BV/TV: Distal Femoral Bone Volume/Total Volume. Tb.N: Trabecular Number. Tb.Th: Trabecular Thickness. Tb.Sp: Trabecular Spacing. M.BV/TV: Midshaft Bone Volume/Total Volume. C.Th: Cortical Thickness.
(PDF)

Figure S3 Representative immunohistochemical/immunofluorescence staining of thyro-parathyroid tissue from *PTH-KL*$^{-/-}$ mice and wild-type controls. A) Proliferation rate as determined by Ki67 index was unaltered in *PTH-KL*$^{-/-}$ mice (40× magnification). B) Dual immunofluorescence staining showed that Klotho co-localized with PTH, CaSR and VDR although the expression level of these proteins appeared quantitatively unaltered in Klotho-deleted cells versus adjacent Klotho-expressing cells (40× magnification).
(PDF)

Figure S4 Calcium – PTH relationship. Mice were injected intraperitoneally with calcium-gluconate or EGTA which causes rapid increments or decrements, respectively, in serum calcium level. Blood samples were drawn after 30 minutes for analysis of serum calcium and PTH. The calcium-PTH relationship in *PTH-KL*$^{-/-}$ mice (n = 8) and wild-type mice (n = 5) is presented and did not differ between the genotypes.
(PDF)

Table S1 Renal gene expression in *PTH-KL*$^{-/-}$ mice and their wild-type littermates. All transcripts were normalized to *Beta-actin*. N = 8 for each genotype.
(PDF)

Table S2 A nanostring array encompassing >90 genes critical for parathyroid function. N = 3 for each genotype. Significant results ($p<0.05$) are in bold.
(PDF)

Table S3 Serum and urine biochemistries in *PTH-KL*$^{-/-}$ and wild-type mice after induction of renal failure.
(PDF)

Acknowledgments

We would like to thank Dr Justin Silver and Dr Tally Naveh-Many at the Hadassah University Hospital, Jerusalem, Israel, for their hospitality and for providing invaluable technical advice.

Author Contributions

Conceived and designed the experiments: HO TEL. Performed the experiments: HO KL RA TS TJ. Analyzed the data: HO TEL. Contributed reagents/materials/analysis tools: RG MM GA BL. Wrote the paper: HO TEL.

References

1. Potts JT (2005) Parathyroid hormone: past and present. J Endocrinol 187: 311–325.
2. Chen RA, Goodman WG (2004) Role of the calcium-sensing receptor in parathyroid gland physiology. Am J Physiol Renal Physiol 286: F1005–1011.
3. Urakawa I, Yamazaki Y, Shimada T, Iijima K, Hasegawa H, et al. (2006) Klotho converts canonical FGF receptor into a specific receptor for FGF23. Nature 444: 770–774.
4. Kuro-o M, Matsumura Y, Aizawa H, Kawaguchi H, Suga T, et al. (1997) Mutation of the mouse klotho gene leads to a syndrome resembling ageing. Nature 390: 45–51.
5. Krajisnik T, Bjorklund P, Marsell R, Ljunggren O, Akerstrom G, et al. (2007) Fibroblast growth factor-23 regulates parathyroid hormone and 1alpha-hydroxylase expression in cultured bovine parathyroid cells. J Endocrinol 195: 125–131.
6. Ben-Dov IZ, Galitzer H, Lavi-Moshayoff V, Goetz R, Kuro-o M, et al. (2007) The parathyroid is a target organ for FGF23 in rats. J Clin Invest 117: 4003–4008.
7. Imura A, Tsuji Y, Murata M, Maeda R, Kubota K, et al. (2007) alpha-Klotho as a regulator of calcium homeostasis. Science 316: 1615–1618.
8. Martuseviciene G, Hofman-Bang J, Clausen T, Olgaard K, Lewin E (2011) The secretory response of parathyroid hormone to acute hypocalcemia in vivo is independent of parathyroid glandular sodium/potassium-ATPase activity. Kidney Int 79: 742–748.
9. Galitzer H, Ben-Dov IZ, Silver J, Naveh-Many T (2010) Parathyroid cell resistance to fibroblast growth factor 23 in secondary hyperparathyroidism of chronic kidney disease. Kidney Int 77: 211–218.
10. Canalejo R, Canalejo A, Martinez-Moreno JM, Rodriguez-Ortiz ME, Estepa JC, et al. (2010) FGF23 fails to inhibit uremic parathyroid glands. J Am Soc Nephrol 21: 1125–1135.
11. Krajisnik T, Olauson H, Mirza MA, Hellman P, Akerstrom G, et al. (2010) Parathyroid Klotho and FGF-receptor 1 expression decline with renal function in hyperparathyroid patients with chronic kidney disease and kidney transplant recipients. Kidney Int 78: 1024–1032.
12. Komaba H, Goto S, Fujii H, Hamada Y, Kobayashi A, et al. (2010) Depressed expression of Klotho and FGF receptor 1 in hyperplastic parathyroid glands from uremic patients. Kidney Int 77: 232–238.
13. Libutti SK, Crabtree JS, Lorang D, Burns AL, Mazzanti C, et al. (2003) Parathyroid gland-specific deletion of the mouse Men1 gene results in parathyroid neoplasia and hypercalcemic hyperparathyroidism. Cancer Res 63: 8022–8028.
14. Imanishi Y, Hall C, Sablosky M, Brown EM, Arnold A (2002) A new method for in vivo analysis of parathyroid hormone-calcium set point in mice. J Bone Miner Res 17: 1656–1661.
15. Jia T, Olauson H, Lindberg K, Amin R, Edvardsson K, et al. (2013) A novel model of adenine-induced tubulointerstitial nephropathy in mice. BMC Nephrol 14: 116.
16. Faul C, Amaral AP, Oskouei B, Hu MC, Sloan A, et al. (2011) FGF23 induces left ventricular hypertrophy. J Clin Invest 121: 4393–4408.
17. Byrd VM, Kilkenny DM, Dikov MM, Reich MB, Rocheleau JV, et al. (2003) Fibroblast growth factor receptor-1 interacts with the T-cell receptor signalling pathway. Immunol Cell Biol 81: 440–450.
18. Goetz R, Mohammadi M (2013) Exploring mechanisms of FGF signalling through the lens of structural biology. Nat Rev Mol Cell Biol 14: 166–180.

19. Sanna B, Brandt EB, Kaiser RA, Pfluger P, Witt SA, et al. (2006) Modulatory calcineurin-interacting proteins 1 and 2 function as calcineurin facilitators in vivo. Proc Natl Acad Sci U S A 103: 7327–7332.
20. Ritter CS, Brown AJ (2011) Direct suppression of Pth gene expression by the vitamin D prohormones doxercalciferol and calcidiol requires the vitamin D receptor. J Mol Endocrinol 46: 63–66.
21. Bell O, Gaberman E, Kilav R, Levi R, Cox KB, et al. (2005) The protein phosphatase calcineurin determines basal parathyroid hormone gene expression. Mol Endocrinol 19: 516–526.
22. Mirza MA, Hansen T, Johansson L, Ahlstrom H, Larsson A, et al. (2009) Relationship between circulating FGF23 and total body atherosclerosis in the community. Nephrol Dial Transplant 24: 3125–3131.
23. Mirza MA, Larsson A, Lind L, Larsson TE (2009) Circulating fibroblast growth factor-23 is associated with vascular dysfunction in the community. Atherosclerosis 205: 385–390.
24. Mirza MA, Larsson A, Melhus H, Lind L, Larsson TE (2009) Serum intact FGF23 associate with left ventricular mass, hypertrophy and geometry in an elderly population. Atherosclerosis 207(2):546–51.
25. Gutierrez OM, Januzzi JL, Isakova T, Laliberte K, Smith K, et al. (2009) Fibroblast growth factor 23 and left ventricular hypertrophy in chronic kidney disease. Circulation 119: 2545–2552.
26. Gutierrez OM, Mannstadt M, Isakova T, Rauh-Hain JA, Tamez H, et al. (2008) Fibroblast growth factor 23 and mortality among patients undergoing hemodialysis. N Engl J Med 359: 584–592.
27. Fliser D, Kollerits B, Neyer U, Ankerst DP, Lhotta K, et al. (2007) Fibroblast growth factor 23 (FGF23) predicts progression of chronic kidney disease: the Mild to Moderate Kidney Disease (MMKD) Study. J Am Soc Nephrol 18: 2600–2608.
28. Lundberg S, Qureshi AR, Olivecrona S, Gunnarsson I, Jacobson SH, et al. (2012) FGF23, albuminuria, and disease progression in patients with chronic IgA nephropathy. Clin J Am Soc Nephrol 7: 727–734.
29. Larsson T, Nisbeth U, Ljunggren O, Juppner H, Jonsson KB (2003) Circulating concentration of FGF-23 increases as renal function declines in patients with chronic kidney disease, but does not change in response to variation in phosphate intake in healthy volunteers. Kidney Int 64: 2272–2279.
30. Lavi-Moshayoff V, Wasserman G, Meir T, Silver J, Naveh-Many T (2010) PTH increases FGF23 gene expression and mediates the high-FGF23 levels of experimental kidney failure: a bone parathyroid feedback loop. Am J Physiol Renal Physiol 299: F882–889.
31. Wolf M (2010) Forging forward with 10 burning questions on FGF23 in kidney disease. J Am Soc Nephrol 21: 1427–1435.
32. Nechama M, Uchida T, Mor Yosef-Levi I, Silver J, Naveh-Many T (2009) The peptidyl-prolyl isomerase Pin1 determines parathyroid hormone mRNA levels and stability in rat models of secondary hyperparathyroidism. J Clin Invest 119: 3102–3114.
33. Olauson H, Lindberg K, Amin R, Jia T, Wernerson A, et al. (2012) Targeted deletion of klotho in kidney distal tubule disrupts mineral metabolism. J Am Soc Nephrol 23: 1641–1651.
34. Harrison BC, Roberts CR, Hood DB, Sweeney M, Gould JM, et al. (2004) The CRM1 nuclear export receptor controls pathological cardiac gene expression. Mol Cell Biol 24: 10636–10649.
35. Goetz R, Nakada Y, Hu MC, Kurosu H, Wang L, et al. (2010) Isolated C-terminal tail of FGF23 alleviates hypophosphatemia by inhibiting FGF23-FGFR-Klotho complex formation. Proc Natl Acad Sci U S A 107: 407–412.
36. Goetz R, Beenken A, Ibrahimi OA, Kalinina J, Olsen SK, et al. (2007) Molecular insights into the klotho-dependent, endocrine mode of action of fibroblast growth factor 19 subfamily members. Mol Cell Biol 27: 3417–3428.

BRIEF COMMUNICATION www.jasn.org

The Kidney Is the Principal Organ Mediating Klotho Effects

Karolina Lindberg,* Risul Amin,* Orson W. Moe,† Ming-Chang Hu,† Reinhold G. Erben,‡ Annika Östman Wernerson,§ Beate Lanske,‖ Hannes Olauson,* and Tobias E. Larsson*¶

*Division of Renal Medicine, Department of Clinical Science, Intervention, and Technology, Karolinska Institutet, Stockholm Sweden; †Charles and Jane Pak Center for Mineral Metabolism and Clinical Research, Department of Internal Medicine, University of Texas Southwestern Medical Center, Dallas, Texas; ‡Department of Biomedical Sciences, University of Veterinary Medicine Vienna, Vienna, Austria; §Division of Pathology, Department of Laboratory Medicine, Karolinska Institutet and Karolinska University Hospital, Stockholm, Sweden; ‖Department of Oral Medicine, Infection, and Immunity, Harvard School of Dental Medicine, Boston, Massachusetts; and ¶Department of Nephrology, Karolinska University Hospital, Stockholm, Sweden

ABSTRACT

Klotho was discovered as an antiaging gene, and α-Klotho (Klotho) is expressed in multiple tissues with a broad set of biologic functions. Membrane-bound Klotho binds fibroblast growth factor 23 (FGF23), but a soluble form of Klotho is also produced by alternative splicing or cleavage of the extracellular domain of the membrane-bound protein. The relative organ-specific contributions to the levels and effects of circulating Klotho remain unknown. We explored these issues by generating a novel mouse strain with Klotho deleted throughout the nephron (*Six2-KL*$^{-/-}$). Klotho shedding from *Six2-KL*$^{-/-}$ kidney explants was undetectable and the serum Klotho level was reduced by approximately 80% in *Six2-KL*$^{-/-}$ mice compared with wild-type littermates. *Six2-KL*$^{-/-}$ mice exhibited severe growth retardation, kyphosis, and premature death, closely resembling the phenotype of systemic *Klotho* knockout mice. Notable biochemical changes included hyperphosphatemia, hypercalcemia, hyperaldosteronism, and elevated levels of 1,25-dihydroxyvitamin D and Fgf23, consistent with disrupted renal Fgf23 signaling. Kidney histology demonstrated interstitial fibrosis and nephrocalcinosis in addition to absent dimorphic tubules. A direct comparative analysis between *Six2-KL*$^{-/-}$ and systemic *Klotho* knockout mice supports extensive, yet indistinguishable, extrarenal organ manifestations. Thus, our data reveal the kidney as the principal contributor of circulating Klotho and Klotho-induced antiaging traits.

J Am Soc Nephrol 25: ●●●–●●●, 2014. doi: 10.1681/ASN.2013111209

Type I membrane-bound α-Klotho (*Klotho*) was originally identified as an antiaging gene based on the senescent phenotype and reduced life span in mice carrying hypomorph *Klotho* alleles (*kl/kl*). *kl/kl* mice exhibit a large spectrum of organ abnormalities such as soft tissue calcifications, osteomalacia, hypogonadism, lung emphysema, and skin atrophy.[1] Although Klotho is expressed in multiple tissues, at the highest level in the kidneys, parathyroid glands, and choroid plexus,[2] its tissue-specific role outside the kidney remains elusive.

Membrane-bound Klotho mediates receptor binding and cell signaling by its ligand fibroblast growth factor-23 (Fgf23).[3] *Fgf23* null mice (*Fgf23*$^{-/-}$) develop a virtually identical phenotype to *kl/kl* mice,[4] including a serum biochemical profile of elevated 1,25-dihydroxyvitamin D [1,25$(OH)_2$D], hypercalcemia, and hyperphosphatemia consistent with disrupted renal Fgf23 signaling. Membrane-bound Klotho can be released by extracellular cleavage and shedding,[5] resulting in its presence in blood, urine, and cerebrospinal fluid, a process at least partially mediated by ADAM10 and ADAM17 (a disintegrin and metalloproteinases 10 and 17, respectively).[6] Soluble Klotho and its endocrine signaling are implicated in diverse biologic processes such as protection of endothelial function, inhibition of phosphate-driven vascular calcification, and suppression of fibrosis and inflammation. The underlying molecular mechanisms are not fully elucidated but involve modulation of Wnt, insulin/IGF1 and TGF-β signaling.[7–9] In addition, soluble Klotho independently promotes renal phosphate excretion and calcium reabsorption by enzymatic modulation of the sodium-dependent phosphate cotransporter 2a (Npt2a) and transient receptor potential cation channel subfamily V member 5, respectively.[10,11]

Received November 20, 2013. Accepted February 26, 2014.

Published online ahead of print. Publication date available at www.jasn.org.

Correspondence: Dr. Tobias E. Larsson, Clinical Research Center, Karolinska University Hospital in Huddinge, Sixth Floor, Novum, SE-141 86 Stockholm, Sweden. Email: tobias.larsson@ki.se

Significant attention was drawn to Klotho biology over the past decade, yet identification of the tissue source of circulating Klotho and the organ-specific contribution to the aging-like phenotype in *kl/kl* mice remain uncertain. We addressed these issues by generating mice with Klotho deleted throughout the nephron (*Six2-KL*$^{-/-}$) using Cre-LoxP recombination (Figure 1, A and B) as described elsewhere.[12] In this model, the Six2 promoter targets expression of Cre recombinase to the cap mesenchyme and its derivatives.[13] In addition, Six2 expression was reported in restricted parts of the hindbrain, esophagus, stomach, and tendons and ligaments of the limbs during embryonal development.[14] Importantly, with the kidney exempt, Six2 expression does not overlap that reported for Klotho. Successful deletion of renal Klotho was confirmed with immunofluorescence and Western blotting (Figure 1, C and D), and renal transcript levels were reduced by approximately 80% compared with wild-type mice (Figure 1E).

Soluble Klotho is present in blood and can be generated by cell membrane shedding or by alternative splicing, the latter presumably less relevant in humans.[5] Regulation of its shedding is a critical step for Klotho function because protection against cellular stressors such as inflammation and oxidative stress is mediated by its endocrine signaling.[7–9] For obvious reasons, it is not feasible to accurately define the tissue source of systemic Klotho in humans. Additional challenges in this regard are that Klotho-deficient conditions, such as CKD, are characterized by a parallel reduction of its tissue level in several Klotho-expressing organs[15–17] and that serum Klotho is potentially modified by differential shedding, the uremic environment, and concurrent comorbidities and medications.

Herein, we characterized Klotho shedding *ex vivo* by using kidney explants and noted undetectable Klotho protein in conditioned media from *Six2-KL*$^{-/-}$ kidneys. By contrast, wild-type kidneys generated substantial amounts of soluble Klotho (Figure 1F). Absent formation of soluble Klotho from *Six2-KL*$^{-/-}$ kidneys was paralleled by a marked reduction (approximately 80%) in the serum Klotho level (Figure 1G). Given the preserved Klotho expression in other key Klotho-expressing tissues (Supplemental Figure 1), it can be concluded that the kidney is the principal source of circulating Klotho and that

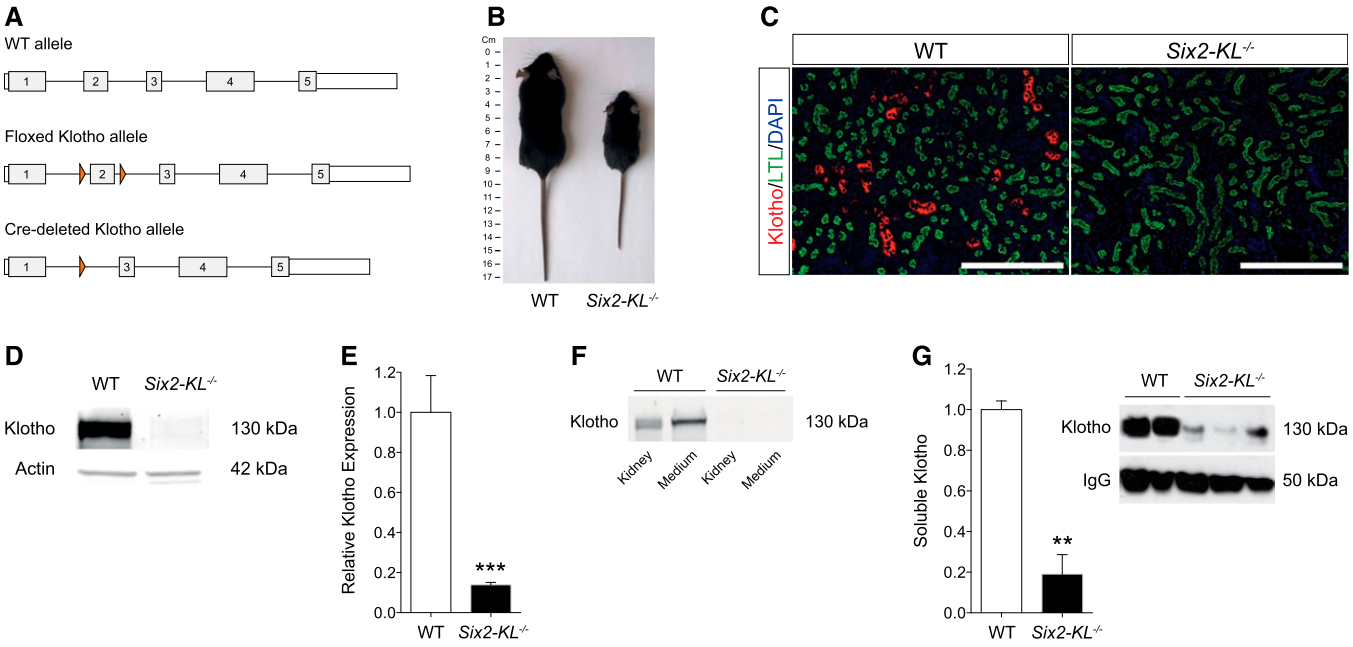

Figure 1. Targeted deletion of Klotho in *Six2-KL*$^{-/-}$ mice. (A) LoxP sequences (red triangles) are introduced in the *Klotho* gene enabling targeted deletion of exon 2 and disruption of gene function. (B) Gross phenotype of 6-week-old wild-type and *Six2-KL*$^{-/-}$ mice. *Six2-KL*$^{-/-}$ mice develop detectable growth retardation and kyphosis at 3 weeks of age. Adult mice display physical inactivity, are infertile, and die prematurely starting at 6–8 weeks of age. (C) Immunofluorescence staining confirms successful deletion of Klotho (red) throughout the nephron in *Six2-KL*$^{-/-}$ mice. LTL (green) is used as a marker of proximal tubules and DAPI (blue) is used for nuclear staining. (D) Western blot on kidney extracts from *Six2-KL*$^{-/-}$ mice confirms successful deletion of renal Klotho protein. (E) Renal Klotho transcripts in *Six2-KL*$^{-/-}$ mice are reduced by approximately 80% compared with wild-type mice as measured with quantitative real-time PCR. (F) Renal Klotho protein shedding is examined *ex vivo*. Klotho protein is readily detected in wild-type kidney homogenates and in conditioned media in which kidney sections are submerged for 2 hours. By contrast, no tissue or shedded Klotho protein is found in kidney explants or media from *Six2-KL*$^{-/-}$ mice. (G) Soluble Klotho is analyzed using immunoprecipitation and Western blot and is reduced by approximately 80% in serum from *Six2-KL*$^{-/-}$ mice. Samples are normalized to IgG. $^{**}P<0.01$; $^{***}P<0.001$. DAPI, 4′,6-diamidino-2-phenylindole; LTL, fluorescein labeled *Lotus tetragonolobus* lectin; WT, wild-type. Bar, 200 μm in C.

other Klotho-expressing organs are incapable of correcting its systemic deficiency. Notably, a short-term small study in healthy kidney donors demonstrated an approximately 30% reduction in serum Klotho 5 days after unilateral nephrectomy,[18] suggesting that our data are transferable to humans.

Six2-KL$^{-/-}$ mice develop growth retardation and kyphosis at 3 weeks of age (Figure 1B and Supplemental Figure 2). Adult mice were infertile, exhibited reduced activity, and died prematurely starting at 6–8 weeks of age, reproducing the reported phenotype of *kl/kl* mice. Serum and urine biochemical parameters were examined at 6 weeks of age (Figure 2, A and B). *Six2-KL*$^{-/-}$ mice had remarkably elevated Fgf23 and 1,25(OH)$_2$D levels in addition to hyperphosphatemia. Parathyroid hormone (PTH) was appropriately decreased in the face of hypercalcemia, whereas aldosterone levels were nearly 3-fold increased. The urine profile showed increased excretion of calcium, whereas phosphate excretion was unchanged. Thus, their biochemical abnormalities largely recapitulate those of *kl/kl* mice and indicate dismantled renal Fgf23 signaling as a result of absent Klotho in the renal tubules. By contrast, heterozygous mice (*Six2-KL*$^{+/-}$) had preserved renal expression of Klotho and were phenotypically normal defined by gross appearance and serum biochemistry profile (data not shown).

Data on renal protein expression and relative expression of renal transcripts are shown in Figure 2, C and D. Immunohistochemical analysis revealed increased expression and relative abundance of Npt2a at the brush border membrane in *Six2-KL*$^{-/-}$ mice, whereas its transcript levels were decreased and dissociated from the protein levels. Transcript levels of the vitamin D activating enzyme Cyp27b1 were increased corroborating with the elevated serum 1,25(OH)$_2$D. The vitamin D inactivating enzyme Cyp24a1 was also increased, presumably as a result of a stimulatory feedback signal from high 1,25(OH)$_2$D, whereas the vitamin D receptor was decreased.

The renal cell proliferation rate (determined by the Ki67 index) was significantly increased in *Six2-KL*$^{-/-}$ mice compared with wild-type mice (1.47% versus 0.57%, $P<0.001$; Figure 2C). The pathophysiologic relevance of this finding warrants further exploration, especially in situations of disturbed tubular-repair mechanisms, but supports data pointing to Klotho as an antiproliferative tumor-suppressor agent.[19]

We next determined the effect of renal Klotho ablation on kidney histology and

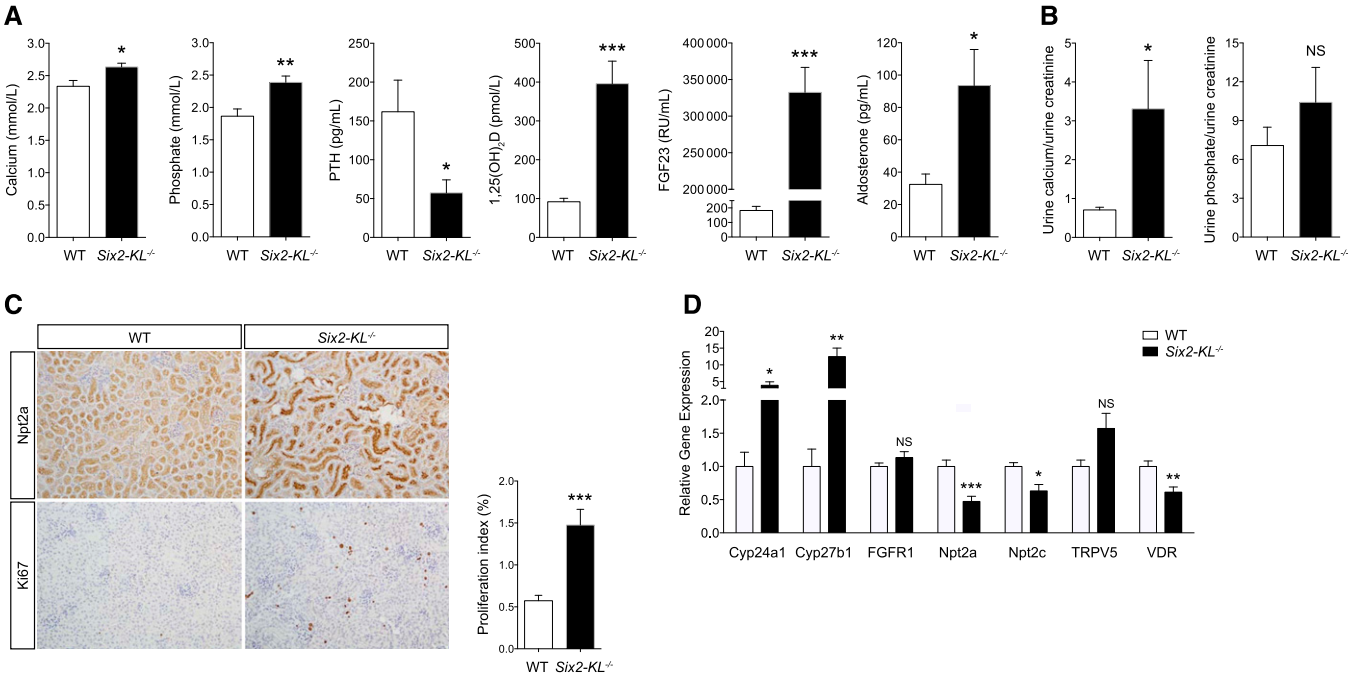

Figure 2. Biochemistry, renal protein, and gene expression in *Six2-KL*$^{-/-}$ mice. (A) Serum parameters are measured at 6 weeks of age. *Six2-KL*$^{-/-}$ mice have extremely elevated Fgf23 and increased serum 1,25(OH)$_2$D, aldosterone, calcium and phosphate, whereas PTH is appropriately decreased. (B) Urine parameters measured at 6 weeks of age show pronounced hypercalcuria in *Six2-KL*$^{-/-}$ mice, whereas phosphate excretion is unaltered compared with wild-type mice. (C) Immunohistochemical staining for Npt2a (top) demonstrates increased protein expression at the brush border membrane in *Six2-KL*$^{-/-}$ mice, corroborating the observed hyperphosphatemia. The proliferation rate determined by Ki67 staining (bottom) is markedly increased in *Six2-KL*$^{-/-}$ mice compared with wild-type controls. (D) Relative expression of renal transcripts. Vitamin D regulating enzymes Cyp27b1 and Cyp24a1 are both increased, whereas the vitamin D receptor is decreased in *Six2-KL*$^{-/-}$ mice. Transcript levels of Npt2a and Npt2c are decreased in *Six2-KL*$^{-/-}$ mice, contrasting the increased protein levels. Expression of TRPV5 and FGFR1 is unaltered. *$P<0.05$; ** $P<0.01$; ***$P<0.001$. $n\geq5$ in each group. FGFR1, FGF receptor 1; TRPV5, transient receptor potential cation channel subfamily V member 5; VDR, vitamin D receptor; WT, wild-type.

detected increased cellular density, loss of differentiation between proximal and distal convoluted tubules, as well as loss of cuboidal epithelium lining Bowman's capsule in male *Six2-KL*$^{-/-}$ mice (consistent with a female phenotype; Figure 3A). This corroborates with the histopathologic evidence for hypoplastic Leydig cells and tubular atrophy in testis (Figure 3B). Additional histomorphologic changes included moderate interstitial fibrosis (Figure 3A) and widespread nephrocalcinosis (Figure 3C). To note, a mosaic deletion of Klotho in the distal tubules did not reproduce these histologic findings in a cell-specific manner (*i.e.*, no fibrosis or calcification was found in Klotho-ablated cells),[12] supporting the concept that the renoprotective effect of Klotho is conveyed by endocrine, rather than autocrine, mechanisms.

A central question is whether extrarenal Klotho, locally or systemically, has a protective role against aging-like traits. *Six2-KL*$^{-/-}$ mice represent a valid model to explore this because they have preserved Klotho expression in other Klotho-expressing organs, such as the parathyroid glands and choroid plexus (Supplemental Figure 1). Accordingly, we conducted an extensive histologic analysis performed by a mouse pathologist to assess potential extrarenal manifestations in *Six2-KL*$^{-/-}$ mice. Ectopic calcifications in soft tissues such as the kidneys, lungs, and arteries demonstrated by von Kossa staining (Figure 3C) were a prominent feature in *Six2-KL*$^{-/-}$ mice. Other notable histologic changes in *Six2-KL*$^{-/-}$ mice included pulmonary emphysema, depletion of periarteriolar lymphoid sheaths, increased red pulp in the spleen, and reduced subcutaneous fat and skin collagen thickness (Figure 3B). These findings are identical with the reported histologic changes in *kl/kl* mice. Bone histology demonstrated hypomineralization in *Six2-KL*$^{-/-}$ mice (Figure 3D), corroborating with peripheral quantitative computed tomography data, showing markedly reduced bone mineral density (Table 1). In summary, at the histologic level, we found diverse and severe extrarenal complications presumably elicited by systemic Klotho deficiency as well as abrogated Fgf23 signaling and abnormalities in mineral metabolism. Indeed, the severe phenotype in *kl/kl* mice is ameliorated by transgenic

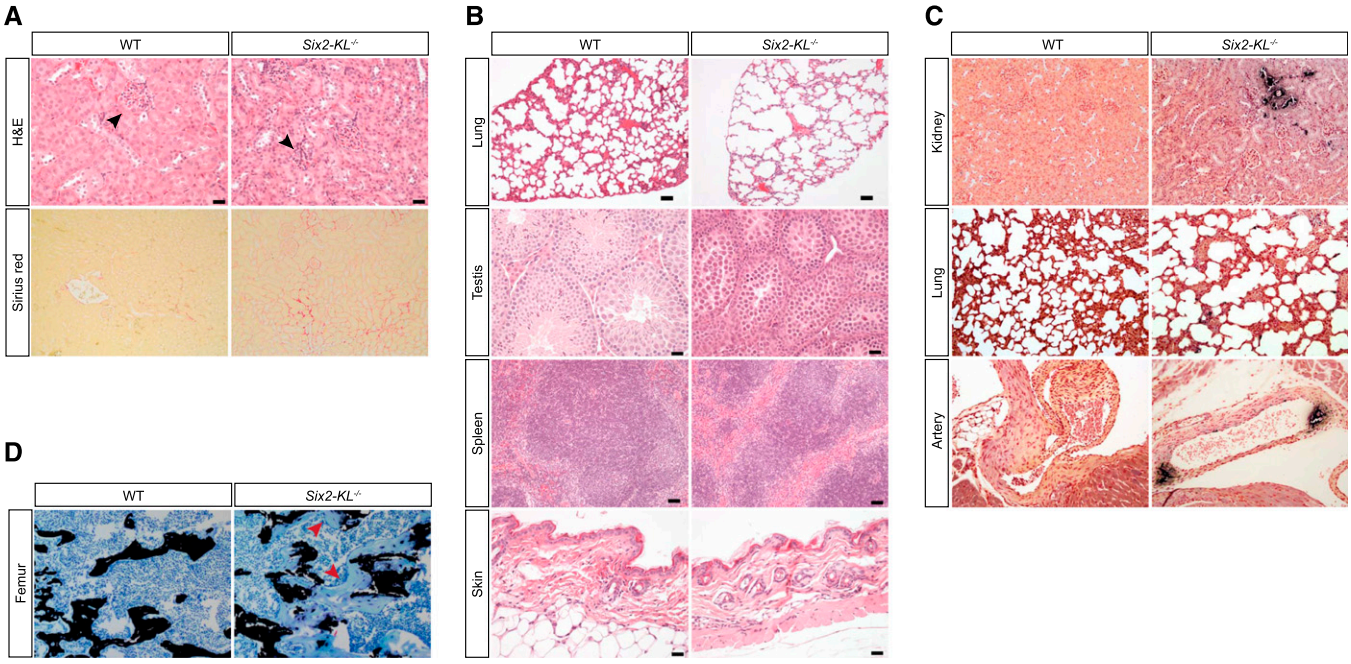

Figure 3. Renal and extrarenal histology in *Six2-KL*$^{-/-}$ mice. (A) Renal morphology is normal in wild-type mice, whereas *Six2- KL*$^{-/-}$ mice have higher cell density and absence of dimorphic tubules (top). A specific feature in male *Six2-KL*$^{-/-}$ mice is the loss of cuboidal Bowman's epithelium of glomeruli (arrowheads). Staining for collagen with Sirius red (bottom) shows a moderate fibrosis in *Six2-KL*$^{-/-}$ mice. (B) The lungs of *Six2-KL*$^{-/-}$ mice have moderate dilation of alveolar spaces and occasional rupture of alveolar septa, consistent with emphysema. Testis of *Six2-KL*$^{-/-}$ mice show marked atrophy, both of tubules and germinative epithelium, and interstitial Leydig cells. Few spermatids and no ripe sperm in *Six2-KL*$^{-/-}$ mice are observed. In the spleen of *Six2-KL*$^{-/-}$ mice, red pulp atrophy is accompanied by a mild increase of interstitial fibrosis and marked depletion of both erythroid and myeloid hematopoietic lineages. The skin of *Six2- KL*$^{-/-}$ mice has no subcutaneous fat with some keratin debris and dysplastic hair shafts. (C) Kidneys (top) from *Six2-KL*$^{-/-}$ mice display widespread tubular and vascular calcifications when stained according to von Kossa. Disseminated calcifications are also found in lungs (middle) and arteries (bottom) from *Six2-KL*$^{-/-}$ mice but not in wild-type mice. (D) *Six2-KL*$^{-/-}$ mice show severe hypomineralization and thickened osteoid seams in the femoral metaphysis (arrowheads) in von Kossa/McNeal–stained, 3-μm–thick, undecalcified sections. H&E, hematoxylin and eosin; WT, wild-type. Bar, 25 μm for testis and skin in B; 50 μm for lung and spleen in B.

Table 1. Bone peripheral quantitative computed tomography in *Six2-KL*$^{-/-}$ mice

Parameter	Wild-Type Mice (*n*=5)	*Six2-KL*$^{-/-}$ Mice (*n*=8)	*P* Value
Total bone mineral density (mg/cm^3)	370.3 (40.7)	272.0 (51.1)	0.001
Trabecular bone mineral density (mg/cm^3)	150.6 (26.0)	101.6 (23.7)	<0.05
Cortical bone mineral density (mg/cm^3)	1017.8 (35.4)	853.6 (74.8)	<0.01
Cortical thickness (mm)	0.172 (0.021)	0.112 (0.020)	<0.001

Data are presented as the mean (SD). Femurs from 6-week-old *Six2-KL*$^{-/-}$ and wild-type controls were collected for analysis. *Six2-KL*$^{-/-}$ mice had significantly reduced cortical and trabecular bone mineral density supporting hypomineralization.

Klotho overexpression and by dietary phosphate and vitamin D restrictions, respectively.[20,21] A limitation of the *Six2-KL*$^{-/-}$ model is the inability to discriminate effects of membrane-bound versus soluble Klotho. Given the severe and early onset of phenotype in *Six2-KL*$^{-/-}$ mice, this issue cannot be appropriately addressed by exogenous Klotho delivery.

The observation that *Six2-KL*$^{-/-}$ mice appear phenotypically indistinguishable from *kl/kl* mice prompted us to perform a direct comparative analysis. To enable this, we generated systemic *Klotho* knockout mice (β*-actin-KL*$^{-/-}$ mice) using mice expressing Cre recombinase under the human β-actin promoter, as previously described.[12] These two strains demonstrated an identical gross phenotype and biochemical profile (Supplemental Figure 3, Supplemental Tables 1 and 2) and extensive histologic analysis did not provide evidence for any differences in renal or extrarenal abnormalities. The hyperaldosteronism in *Six2-KL*$^{-/-}$ mice further strengthens the concept that endocrine manifestations in *kl/kl* mice are caused by the systemic environment, rather than local Klotho expression. Taken together, our data unequivocally point to the kidney as the prime mediator of Klotho function.

Our novel findings have several implications. CKD is a state of Klotho deficiency and we for the first time demonstrate that reduced Klotho in the kidney has a dramatic effect on its systemic availability and presumed endocrine signaling. Reduced Klotho abundance in the kidney may therefore directly contribute to complications such as renal fibrosis, progressive loss of kidney function, and cardiovascular dysfunction frequently observed in CKD.[16,22] In support of this, systemic Klotho treatment in experimental CKD models improves uremic complications such as matrix deposition, renal fibrosis, osteogenic transformation of vascular smooth muscle cells, and vascular calcification.[9,23] By combining this knowledge with our present findings, therapeutic Klotho delivery, or augmentation of its endocrine functions, may be a feasible option to mitigate organ damage and slow disease progression in patients with CKD.

CONCISE METHODS

Ethical Statement

All experiments were conducted in compliance with the guidelines of animal experiments at Karolinska Institutet and were approved by Stockholm South Animal Experimental Ethical Committee (permit number S 38-09, S 68-10). Mice were fed standard rodent chow (RM1; SDS Special Diet Services, Essex, UK) containing 0.73% calcium and 0.52% phosphorous. All animals had free access to food and drinking water and were housed in standard makrolon cages with wood chip bedding and a paper house for enrichment, at constant ambient temperature (21°C–22°C) and humidity (40%–50%).

Generation of Kidney-Specific Klotho Knockout Mice

Mice with tissue-specific Klotho deletion were generated using Cre-Lox recombination as previously described.[12] Briefly, loxP sequences were introduced in the flanking regions of exon 2 of the *Klotho* gene, resulting in a nonfunctioning Klotho protein in tissues expressing Cre recombinase. Floxed Klotho mice were crossed with mice expressing Cre recombinase under the Six2 promoter [Tg (Six2-EGFP/cre)1Amc/J; The Jackson Laboratory, Bar Harbor, ME] or under the human β-actin promoter [FVB/N-Tg(ACTB-cre) 2Mrt/J; The Jackson Laboratory] to generate kidney-specific and systemic Klotho knockout mice, respectively. Floxed Klotho mice not expressing Cre served as wild-type controls. All strains were kept on a C57BL/6 background.

Genotyping

Total DNA was extracted from tail biopsies (ViaGen, Cedar Park, TX) and PCR amplification was carried out (Qiagen, Venlo, The Netherlands).

Serum Biochemistries

Serum calcium, phosphate, and creatinine were measured using quantitative colorimetric assay kits (BioAssay; BioChain Institute, Inc., Newark, CA). Serum PTH was measured using the mouse 1-84 PTH ELISA and FGF23 was measured using the mouse FGF23 (c-term) ELISA (Immutopics, San Clemente, CA). Serum $1,25(OH)_2D$ was measured using the EIA assay (Immunodiagnostic Systems, Scottsdale, AZ). Serum aldosterone was measured using a ELISA (Enzo Life Sciences, Farmingdale, NY).

Transcript Analyses

Kidneys were homogenized (Qiagen) and total RNA was extracted (Omega Bio-Tek, Norcross, GA). DNA was removed (Omega Bio-Tek) and first-strand cDNA was synthesized (Bio-Rad, Hercules, CA). Quantitative real-time PCR analysis was performed using a SYBR Green–based assay (Bio-Rad). The relative gene expression was calculated with the $2^{-\Delta\Delta}$ method normalizing the gene of interest to β-actin in the same sample.

Western Blot Analyses

Kidneys were homogenized and extracts were centrifuged. Protein quantification was carried out before blotting (Thermo Fisher Scientific, Waltham, MA). Forty micrograms of protein was separated and electrotransferred

(Invitrogen, Carlsbad, CA). After blocking, the membranes were sequentially incubated with primary and secondary antibodies. Primary antibodies were anti-Klotho (KM2076; TransGenic, Inc., Kobe, Japan) and anti–β-actin (Sigma-Aldrich, St. Louis, MO), and secondary antibodies were from LI-COR Bioscience (Lincoln, NE).

Immunohistochemistry and Immunofluorescence

Tissues were dissected, fixed in 4% paraformaldehyde overnight, and subsequently embedded in paraffin. Four-micrometer sections were deparaffinized, rehydrated, and incubated with low-pH antigen unmasking solution (Vector Laboratories, Burlingame, CA). Sections for immunohistochemistry were then immersed in 3% H_2O_2 in methanol, treated with 4% normal serum, and blocked with avidin and biotin (Vector Laboratories). All sections were incubated with primary antibodies at 4°C overnight. Immunohistochemistry slides were incubated with biotinylated secondary antibodies followed by Vector ABC Reagent and developed with 3,3′-diaminobenzidine substrate (Vector Laboratories). For immunofluorescence, Alexa Fluor conjugated secondary antibodies were used for visualization (Invitrogen) together with fluorescein labeled *Lotus tetragonolobus* lectin, a marker of proximal tubules (Vector Laboratories). For nuclear staining, 4′,6-diamidino-2-phenylindole (Invitrogen) was used. The primary antibodies used were anti-Klotho (KM2076), rabbit monoclonal anti-Ki67 (SP6; Thermo Fisher Scientific), and rabbit polyclonal anti-Npt2a (NPT27; Alpha Diagnostic, Inc., San Antonio, TX). The proliferation index (%) was calculated as the number of Ki67-positive cells/total number of cells in at least four viewing fields (at $\times$10 magnification) from two sections of each assessed mouse.

Histology

Paraffin sections from wild-type and *Six2-KL*$^{-/-}$ mice were stained with hematoxylin and eosin and examined in a blinded fashion by a animal pathologist. Renal sections were stained with Picrosirius red for fibrosis (stains collagen I and III fibers) and were examined by a blinded renal pathologist. Soft tissues were stained with von Kossa to detect calcification.

Bone Phenotype

Processing of undecalcified bone specimens and cancellous bone histology in the distal femoral metaphysis were performed as described elsewhere.[24,25] The area within 0.25 mm from the growth plate was excluded from the measurements. Bone mineral density and other parameters of interest were analyzed by peripheral quantitative computerized tomography using a Scanco Medical μCT 35 system (Scanco USA, Inc., Wayne, PA).

Ex Vivo Study of Secreted Klotho

Mice were anesthetized and perfused with warm 199 medium (Gibco, Grand Island, NY). Kidneys were rapidly harvested, sliced in four equal pieces, and submerged in prewarmed 199 cell medium for 2 hours at 37° with 5% CO_2 and 95% O_2, after which the kidneys and medium were harvested.

Serum Klotho Measurements

Soluble Klotho in serum was measured by a combination of immunoprecipitation and Western blotting as described elsewhere.[16,23]

Statistical Analyses

GraphPad Prism 6.0 (GraphPad Software, Inc., La Jolla, CA) was used for statistical analysis. Gaussian distribution was tested using the D'Agostino and Pearson omnibus normality test. Variables fulfilling the criteria for normal distribution were tested with the two-tailed *t* test. Non-normally distributed variables were compared using the Mann–Whitney test. *P* values <0.05 were considered statistically significant.

ACKNOWLEDGMENTS

We thank Christina Hammarstedt, Christiane Schüler, and Claudia Bergow for valuable technical assistance, and Raoul Kuiper for assisting with extensive morphologic phenotyping.

This work was supported by the Swedish Foundation for Strategic Research, the Swedish Research Council, the Swedish Kidney Foundation, and grants from the Karolinska Institutet and Karolinska University Hospital. The funders had no role in the study design, data collection and analysis, decision to publish, or preparation of the manuscript.

DISCLOSURES

T.E.L. is a Medical Director at Astellas Pharma.

REFERENCES

1. Kuro-o M, Matsumura Y, Aizawa H, Kawaguchi H, Suga T, Utsugi T, Ohyama Y, Kurabayashi M, Kaname T, Kume E, Iwasaki H, Iida A, Shiraki-Iida T, Nishikawa S, Nagai R, Nabeshima YI: Mutation of the mouse klotho gene leads to a syndrome resembling ageing. *Nature* 390: 45–51, 1997
2. Li SA, Watanabe M, Yamada H, Nagai A, Kinuta M, Takei K: Immunohistochemical localization of Klotho protein in brain, kidney, and reproductive organs of mice. *Cell Struct Funct* 29: 91–99, 2004
3. Urakawa I, Yamazaki Y, Shimada T, Iijima K, Hasegawa H, Okawa K, Fujita T, Fukumoto S, Yamashita T: Klotho converts canonical FGF receptor into a specific receptor for FGF23. *Nature* 444: 770–774, 2006
4. Shimada T, Kakitani M, Yamazaki Y, Hasegawa H, Takeuchi Y, Fujita T, Fukumoto S, Tomizuka K, Yamashita T: Targeted ablation of Fgf23 demonstrates an essential physiological role of FGF23 in phosphate and vitamin D metabolism. *J Clin Invest* 113: 561–568, 2004
5. Matsumura Y, Aizawa H, Shiraki-Iida T, Nagai R, Kuro-o M, Nabeshima Y: Identification of the human klotho gene and its two transcripts encoding membrane and secreted klotho protein. *Biochem Biophys Res Commun* 242: 626–630, 1998
6. Chen CD, Podvin S, Gillespie E, Leeman SE, Abraham CR: Insulin stimulates the cleavage and release of the extracellular domain of Klotho by ADAM10 and ADAM17. *Proc Natl Acad Sci U S A* 104: 19796–19801, 2007
7. Kurosu H, Yamamoto M, Clark JD, Pastor JV, Nandi A, Gurnani P, McGuinness OP, Chikuda H, Yamaguchi M, Kawaguchi H, Shimomura I, Takayama Y, Herz J, Kahn CR, Rosenblatt KP, Kuro-o M: Suppression of aging in mice by the hormone Klotho. *Science* 309: 1829–1833, 2005
8. Liu H, Fergusson MM, Castilho RM, Liu J, Cao L, Chen J, Malide D, Rovira II, Schimel D, Kuo CJ, Gutkind JS, Hwang PM, Finkel T: Augmented Wnt signaling in a mammalian model of accelerated aging. *Science* 317: 803–806, 2007
9. Doi S, Zou Y, Togao O, Pastor JV, John GB, Wang L, Shiizaki K, Gotschall R, Schiavi S, Yorioka N, Takahashi M, Boothman DA, Kuro-o M: Klotho inhibits transforming growth factor-beta1 (TGF-beta1) signaling and suppresses renal fibrosis and cancer metastasis in mice. *J Biol Chem* 286: 8655–8665, 2011
10. Chang Q, Hoefs S, van der Kemp AW, Topala CN, Bindels RJ, Hoenderop JG: The beta-glucuronidase klotho hydrolyzes and activates the TRPV5 channel. *Science* 310: 490–493, 2005

11. Hu MC, Shi M, Zhang J, Pastor J, Nakatani T, Lanske B, Razzaque MS, Rosenblatt KP, Baum MG, Kuro-o M, Moe OW: Klotho: A novel phosphaturic substance acting as an autocrine enzyme in the renal proximal tubule. *FASEB J* 24: 3438–3450, 2010
12. Olauson H, Lindberg K, Amin R, Jia T, Wernerson A, Andersson G, Larsson TE: Targeted deletion of Klotho in kidney distal tubule disrupts mineral metabolism. *J Am Soc Nephrol* 23: 1641–1651, 2012
13. Kobayashi A, Valerius MT, Mugford JW, Carroll TJ, Self M, Oliver G, McMahon AP: Six2 defines and regulates a multipotent self-renewing nephron progenitor population throughout mammalian kidney development. *Cell Stem Cell* 3: 169–181, 2008
14. Oliver G, Wehr R, Jenkins NA, Copeland NG, Cheyette BN, Hartenstein V, Zipursky SL, Gruss P: Homeobox genes and connective tissue patterning. *Development* 121: 693–705, 1995
15. Krajisnik T, Olauson H, Mirza MA, Hellman P, Akerström G, Westin G, Larsson TE, Björklund P: Parathyroid Klotho and FGF-receptor 1 expression decline with renal function in hyperparathyroid patients with chronic kidney disease and kidney transplant recipients. *Kidney Int* 78: 1024–1032, 2010
16. Hu MC, Shi M, Zhang J, Quiñones H, Griffith C, Kuro-o M, Moe OW: Klotho deficiency causes vascular calcification in chronic kidney disease. *J Am Soc Nephrol* 22: 124–136, 2011
17. Komaba H, Goto S, Fujii H, Hamada Y, Kobayashi A, Shibuya K, Tominaga Y, Otsuki N, Nibu K, Nakagawa K, Tsugawa N, Okano T, Kitazawa R, Fukagawa M, Kita T: Depressed expression of Klotho and FGF receptor 1 in hyperplastic parathyroid glands from uremic patients. *Kidney Int* 77: 232–238, 2010
18. Akimoto T, Kimura T, Watanabe Y, Ishikawa N, Iwazu Y, Saito O, Muto S, Yagisawa T, Kusano E: The impact of nephrectomy and renal transplantation on serum levels of soluble Klotho protein. *Transplant Proc* 45: 134–136, 2013
19. Wolf I, Levanon-Cohen S, Bose S, Ligumsky H, Sredni B, Kanety H, Kuro-o M, Karlan B, Kaufman B, Koeffler HP, Rubinek T: Klotho: A tumor suppressor and a modulator of the IGF-1 and FGF pathways in human breast cancer. *Oncogene* 27: 7094–7105, 2008
20. Masuda H, Chikuda H, Suga T, Kawaguchi H, Kuro-o M: Regulation of multiple ageing-like phenotypes by inducible klotho gene expression in klotho mutant mice. *Mech Ageing Dev* 126: 1274–1283, 2005
21. Ohnishi M, Razzaque MS: Dietary and genetic evidence for phosphate toxicity accelerating mammalian aging. *FASEB J* 24: 3562–3571, 2010
22. Satoh M, Nagasu H, Morita Y, Yamaguchi TP, Kanwar YS, Kashihara N: Klotho protects against mouse renal fibrosis by inhibiting Wnt signaling. *Am J Physiol Renal Physiol* 303: F1641–F1651, 2012
23. Hu MC, Shi M, Zhang J, Quiñones H, Kuro-o M, Moe OW: Klotho deficiency is an early biomarker of renal ischemia-reperfusion injury and its replacement is protective. *Kidney Int* 78: 1240–1251, 2010
24. Hofbauer LC, Zeitz U, Schoppet M, Skalicky M, Schüler C, Stolina M, Kostenuik PJ, Erben RG: Prevention of glucocorticoid-induced bone loss in mice by inhibition of RANKL. *Arthritis Rheum* 60: 1427–1437, 2009
25. Erben RG: Embedding of bone samples in methylmethacrylate: An improved method suitable for bone histomorphometry, histochemistry, and immunohistochemistry. *J Histochem Cytochem* 45: 307–313, 1997

This article contains supplemental material online at http://jasn.asnjournals.org/lookup/suppl/doi:10.1681/ASN.2013111209/-/DCSupplemental.